

# **Review of 'Impact of Multiple Radar reflectivity data assimilation on the numerical simulation of a Flash Flood Event during the HyMeX campaign' by Maiello et al.**

## **Responses to referee#2**

### **General comments**

The authors have improved their manuscript by clarifying their goal and their contribution to the field of hydro-meteorological research. I am pleased to read that the authors 'accept the advice to go deeply into the meteorology of the event to see which is its interaction with the data assimilation method'. However, I do not see much evidence of it in the revised manuscript. My opinion is that without any clear statistical significance (see below my comment regarding confidence intervals) or in-depth analysis of the data assimilation process, the manuscript fails to meet publication standards.

We thank again the reviewer for the useful comments. The authors worked on the manuscript to provide a clearer statistical significance (the results have been interpreted in the light of bootstrap confidence intervals) and trying to go more in-depth into the assimilation process. Please refer to the answers below and to the modifications in the manuscript highlighted in green.

Moreover, some other appropriate references have been included in the text and also the presentation quality has been improved (some sections have been rearranged in a well structured way and English language has been corrected).

### **Specific comments**

**Subsection 3.1:** In my previous review, I asked for more details regarding the assimilated radar observations. I still do not understand what exactly is being done. The authors replied that no thinning was performed. I think that this piece of information should be mentioned in the text. I do not know what 'model format' means (l 171). Does it mean that the radar data are interpolated onto the model grid? If yes, how? Is there any smoothing? What is the minimum assimilated reflectivity? Does it depend on the range? It should be added in the text that pixels affected by partial beam blockage have been removed, as mentioned by the authors in their reply to one of my comments.

Subsection 3.1 has been rearranged mentioning in the text more details about the assimilated radar observations, the piece of information about thinning has been added to the text, the sentence l171 has been better explained and also the information concerning the partial beam blockage has been included into the manuscript.

Following we tried to explain the meaning of the sentence in line 171:

Volume reflectivity radar data, for each elevation, are converted onto the Cartesian plane in order to find the closest radar bin for each Cartesian grid point. Then, they are interpolated by the 3D-Var code of WRF.

No smoothing or superrobbing is applied.

The minimum assimilated reflectivity is related to the minimum detectable reflectivity (MDZ) that depends on the distance as well as the technical parameters of each radar system. Anyway a minimum threshold is set to -20 dBZ.

In addition, due to the fact that non conventional data such as radar data (or for instance also radiance and rainfall data) don't go through the OBSPROC procedure, they require separate pre-processing. Because radar data comes in a variety of different formats, it is the user's responsibility to convert their data into this format. For 3D-Var, these observations should be placed in a file named *ob.radar*. So it was necessary to write an ad hoc shell script in Fortran language to convert the native radar format into the proper format (a text-based format) for the ingestion into the 3D-Var. This format is showed following:

TOTAL NUMBER = 16		Name of radar	Lat&lon of radar	Altitude of radar	date	
RADAR	KCYS	-104.806	41.152	1887.0	2015-07-07_21:00:00	
						5497
						11
						Total # of sounding
						# of elevations
						3 elevations
altitude						3 elevations
RV						Lat & lon of data
QC index						RF
Err variance						
FM-128 RADAR		2015-07-07_21:00:00	41.165	-107.189	1887.0	
3735.9 -888888.000 -88 -888888.000			10.288	0	0.576	
5128.9 -888888.000 -88 -888888.000			13.029	0	0.944	
6870.5 -888888.000 -88 -888888.000			8.192	0	1.229	
FM-128 RADAR		2015-07-07_21:00:00	41.192	-107.189	1887.0	
3737.3 -888888.000 -88 -888888.000			10.262	0	0.746	
5130.6 -888888.000 -88 -888888.000			13.338	0	0.473	
6872.5 -888888.000 -88 -888888.000			8.373	0	0.626	
FM-128 RADAR		2015-07-07_21:00:00	41.219	-107.189	1887.0	
3740.0 -888888.000 -88 -888888.000			9.447	0	1.072	
5133.9 -8.476 0 1.632			12.828	0	0.833	
6876.7 -888888.000 -88 -888888.000			8.969	0	0.991	
FM-128 RADAR		2015-07-07_21:00:00	41.246	-107.189	1887.0	
3744.2 -888888.000 -88 -888888.000			12.750	0	1.918	
5139.0 -888888.000 -88 -888888.000			15.127	0	0.948	
6883.0 -888888.000 -88 -888888.000			11.409	0	0.932	
FM-128 RADAR		2015-07-07_21:00:00	41.138	-107.153	1887.0	
3645.0 -888888.000 -88 -888888.000			11.011	0	0.882	
5017.0 -888888.000 -88 -888888.000			12.650	0	0.879	
6732.4 -888888.000 -88 -888888.000			6.896	0	1.287	
FM-128 RADAR		2015-07-07_21:00:00	41.165	-107.153	1887.0	
3645.0 -888888.000 -88 -888888.000			11.477	0	0.804	
5017.0 -5.278 0 1.641			13.550	0	0.990	
6732.4 -888888.000 -88 -888888.000			9.280	0	2.035	
FM-128 RADAR		2015-07-07_21:00:00	41.192	-107.153	1887.0	
3646.4 -0.267 0 4.448			11.606	0	1.225	
5018.7 -5.217 0 1.843			14.294	0	0.731	
6734.5 -888888.000 -88 -888888.000			10.094	0	2.072	

### Subsection 3.1 has been modified as follows:

Conventional observations SYNOP and TEMP were retrieved from the ECMWF Meteorological Archival and Retrieval System (MARS). They have been packed in a suitable format for ingest into the assimilation procedure using the Observation Preprocessor (OBSPROC) module provided by the 3D-Var system. Among its main functions there are also to perform a quality control check and to assign observational errors based on a pre-specified error file. In short, a total of 983 observations (967 SYNOP and 16 TEMP) are ingested into the coarse resolution domain, whereas a total of 338 (333 SYNOP and 5 TEMP) observations into the high resolution one.

Reflectivity volumes taken from three C-band Doppler radars operational during the IOP4 have been assimilated to improve IC. The radars have different technical characteristics and were operated with different scanning strategies and operational settings as shown in Table 1.

Monte Midia (MM) and San Pietro Capofiume (SPC) radars are included in the Italian weather radar network, while Polar 55C (P55C) radar is a research radar working on demand, but was operational during the IOPs of the HyMeX campaign (Roberto et al., 2016).

It is worth mentioning that radar data can be affected by numerous sources of errors, mainly due to ground clutter, attenuation due to propagation or beam blocking, anomalous propagation and radio interferences. This is the reason why a preliminary "cleaning" procedure is applied to the measured radar reflectivity from the three radars before the assimilation process, consisting of the following 3 steps:

- a first quality check of radar volumes to filter out radar pixels affected by ground clutter and anomalous propagation. Furthermore, Z was corrected for attenuation using a methodology based on the specific differential phase shift ( $K_{dp}$ ) available for dual polarization radars (Vulpiani et al., 2015); moreover, reflectivity is not corrected for partial beam blocking : all the data that are affected by partial beam blocking and clutter have been filtered out;

- volume reflectivity radar data, for each elevation, are projected onto the Cartesian plane in order to find the closest radar bin for each Cartesian grid point and then they are interpolated by the 3D-Var code of WRF;
- the minimum assimilated reflectivity is set to -20 dBZ;

After the pre-processing procedure, a conversion from the native radar format into the one requested for the ingestion into the 3D-Var is applied to all radars reflectivity data.

Moreover, no observation thinning is performed because this procedure is not yet developed into the 3D-Var system for radar data. Nevertheless, a dynamical thinning has been devised that selects, for every assimilation cycle, the most influential partition of a particular measurement, from information based on the previous cycle: this is the multiple outer loops technique explained later in Section 4.

- II 219-222:** The reader wonders which experiment is actually selected. I suggest moving the contents of Subsection 4.1 right after II 219-222 (and remove the subsectioning of Section 4 or rename the current Subsection 4.2 as a new Section 5). So that MET is already introduced, II 239-245 could form the contents of a Subsection 3.3 titled, eg, 'Evaluation'.

We agree with the reviewer, the modifications suggested can improve the reading of the manuscript, therefore the content of subsection 4.1 have been moved after II 219-222 and subsection 4.2 has been renamed as a new Section 5. Moreover, II 239-245 formed the contents of a new Subsection 3.3 titled "Evaluation" where an overview of MET tool and bootstrap confidence intervals method have been done.

- II 264-266:** The details given by the authors regarding how the statistical indices are computed ('The 12 hours accumulations have been calculated from the 2012-09-14 12:00:00 to 2012-09-16 00:00 every 6 hours') should be added to the text.

The details regarding how the statistical indices are computed have been added to the text as follows (the authors decided to substitute the old figure 7 with a new table 4 that summarizes the realized scores):

In Table 4 statistical indices ACC, FBIAS, ETS and FAR are reported, with their relative upper and lower confidence limits for the 12 hours accumulated precipitation and for two thresholds of precipitation: 1 mm/12h and 40 mm/12h, light and heavy rain regimes, respectively. These two thresholds have been chosen due to their higher statistical significance than the other ones.

We obtained likely good values for ACC and FAR for all the experiments and for heavy rain regimes, strengthened by a small uncertainty interval. On the other hand, for the lower threshold it can be seen that for all simulations the values of FBIAS considering also the confidence intervals are greater than one. One possible interpretation of the impact of the lower threshold, is that with 95% confidence all the experiments are overestimating the frequency of precipitation around 1 mm/12h.

It seems that MET also provides bootstrap confidence intervals. It would be useful to consider them when discussing the results.

For the calculation of MET statistical indices the bootstrap confidence intervals (CIs 95%) have been used.

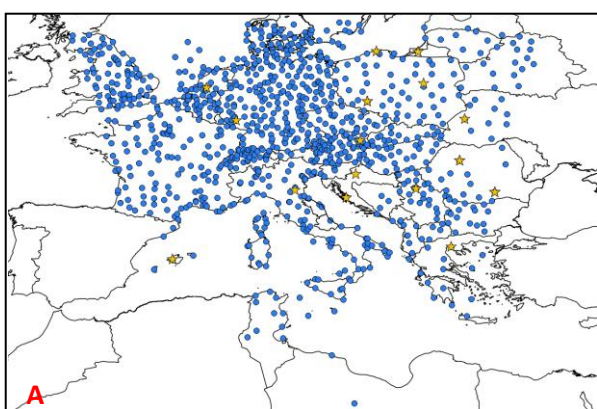
The values of any statistic are realizations from a population of possible values and single summary scores gives only an indication of the forecast performance, whereas the CIs give us information about how much aleatoric (or sampling) uncertainty we have. Providing and discussing CIs can strengthen the results in the sense that they provide uncertainty information, which gives us a better idea about whether or not, in this case, the values obtained are likely good or bad.

- **II 292-293:** I still do not understand why CON 3KM is worse than CTL (it seems quite obvious from Table 5 or Table 7). The authors explain that there are only few data ingested in the smaller domain. But it is anyway more than no data as in CTL, isn't it? Also, why does data assimilation in both domains (experiment CON 12KM 3KM) produce low statistics compared to no assimilation at all (CTL) or assimilation in the coarser resolution domain only (CON HR 12KM)?

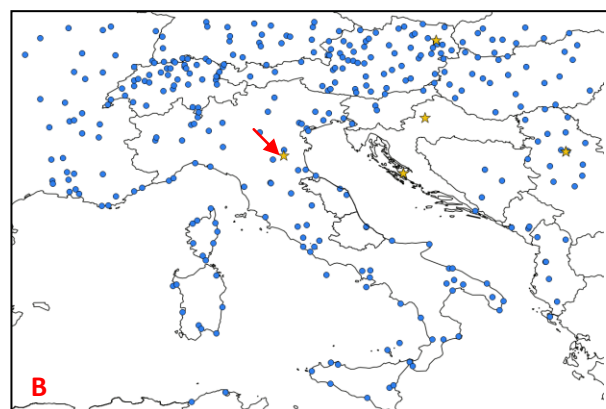
The doubts of the reviewer would be reasonable, although in these lines we were focusing the attention on the impact of the assimilation at different resolution and not on the impact of different types of observations.

Anyway, it is evident from the images below how only one of the 5 total TEMP (yellow stars) falls into the 3 km domain (figure B) and also how far it is from where the event occurred: this is the sounding of Bologna in Emilia Romagna region. Furthermore, looking at Abruzzo and Marche regions, or central Italy in general, there is a low density of surface stations. It has to be reminded that most of these observations have already been used by ECMWF to produce their analysis and that they are here used as first guess, even if at lower resolution ( $0.25^\circ$ ): therefore, they come to be correlated to the background and the improvements of those experiments where they are assimilated are expected to be low. For this reason we couldn't expect a large improvement in the DA experiments where both SYNOP and TEMP have been assimilated. As explained by Liu and Rabier (2002) in their paper entitled "The interaction between model resolution, observations resolution and observations density in data assimilation: a one-dimensional study", the correct balance among the model resolution, the observation density and the observation resolution is crucial for a good initialization. In their paper Liu and Rabier used a synthetic set of data, varying the density and resolution in a one dimensional case: they found that for these observations having a spatial error correlation, the thinning process could help to find a good compromise between the data density and correlation, producing a good analysis accuracy. In our work the bi-dimensional data density (SYNOP) is well larger than that of the three-dimensional ones (TEMP). So the poor results obtained assimilating conventional observations probably depend on the large difference between the spatial density and the number of surface bi-dimensional and three-dimensional data of radiosondes.

The above considerations have been also added to the manuscript at the end of new section 5.



967 SYNOP (dots) + 16 TEMP (stars) on D01 - 00UTC 14 SEPT 2012



331 SYNOP (dots) + 5 TEMP (stars) on D02- 00UTC 14 SEPT 2012

- **Fig.1:** The source of the data (most likely analyses of a global model, I suppose) should be mentioned.

We agree with the reviewer. The caption of figure 1 has been modified as follows:

"Figure 1. ECMWF (European Center for Medium-Range Weather Forecasts) analyses at 12:00UTC on 14 September 2012: a) mean sea level pressure, c) temperature (color shades) and geopotential height (black isolines) at 500 hPa; ECMWF analyses at 12:00UTC on 15 September 2012: b) mean sea level pressure, d) temperature (black isolines) and geopotential height (color shades) at 500 hPa."

- **Table 2:** Points ('.') should be used instead of commas (',') as decimal separators. The SI symbol for kilometre is 'km', not 'Km'. Degree symbols ("°") should be added after elevation angles (I suppose degrees are actually used here).

I suppose the reviewer means Table 1 instead of Table 2. Commas (',') as decimal separators have been replaced by points ('.'): the SI symbol for kilometre became "km"; degree symbols ("°") have been added after elevation angles.

**Table 1: Technical characteristics of the three radars whose reflectivity have been assimilated during IOP4.**

Features	Units	MM radar	P55C radar	SPC Radar
Owner		CF Abruzzo Region	ISAC-CNR of Rome	Arpa Emilia Romagna
Location		Monte Midia	Rome	San Pietro Capofiume
Latitude	[deg]	42.057	41.840	44.6547
Longitude	[deg]	13.177	12.647	11.6236
Height (a.s.l.)	[m]	1760	130	31
Doppler		YES	YES	YES
Dual Polarization		NO	YES	YES
Range Resolution	[m]	500	75	250
Temporal Resolution	[min]	15	5	15
Number of PPI scans	[°]	4 (0, 1, 2, 3)	6 or 8 (0.6, 1.6, 2.6, 4.4, 6.2, 8.3, 11.0, 14.6)	6 (0.53, 1.4, 2.3, 3.2, 4.15, 5.0)
Maximum Range	[km]	120 or 240	125	125

# Impact of Multiple Radar reflectivity data assimilation on the numerical simulation of a Flash Flood Event during the HyMeX campaign

Ida Maiello<sup>1</sup>, Sabrina Gentile<sup>2,1</sup>, Rossella Ferretti<sup>3</sup>, Luca Baldini<sup>3</sup>, Nicoletta Roberto<sup>3</sup>, Errico Picciotti<sup>4,1</sup>, Pier Paolo Alberoni<sup>4</sup>, Frank Silvio Marzano<sup>4,1</sup>

<sup>1</sup>CETEMPS, Department of Physical and Chemical Sciences - University of L'Aquila, L'Aquila, Italy

<sup>2</sup> Institute of Methodologies for Environmental Analysis, CNR IMAA, Potenza, Italy

<sup>3</sup>Institute of Atmospheric Sciences and Climate, CNR ISAC, Roma, Italy

<sup>4</sup>Himet s.r.l, L'Aquila, Italy

<sup>5</sup>ArpaE Emilia Romagna - Servizio Idro-Meteo-Clima, Bologna, Italy

<sup>6</sup>Department of Electronic Engineering, Sapienza University of Rome, Rome, Italy

*Correspondence to:* Ida Maiello (ida.maiello@aquila.infn.it)

**Abstract.** An analysis to evaluate the impact of multiple radar reflectivity data with a three dimensional variational (3D-Var) assimilation system on a heavy precipitation event is presented. The main goal is to build a regionally-tuned numerical prediction model and a decision-support system for environmental civil protection services and demonstrate it in the central Italian regions, distinguishing which type of observations, conventional and not (or a combination of them) is more effective in improving the accuracy of the forecasted rainfall. In that respect, during the first Special Observation Period (SOP1) of HyMeX (Hydrological cycle in the Mediterranean Experiment) campaign several Intensive Observing Periods (IOPs) were launched and nine of which occurred in Italy. Among them, IOP4 is chosen for this study because of its low predictability regarding the exact location and amount of precipitation. This event hit central Italy on 14 September 2012 producing heavy precipitation and causing several damages to buildings, infrastructures and roads. Reflectivity data taken from three C-band Doppler radars running operationally during the event are assimilated using 3D-Var technique to improve high resolution initial conditions. In order to evaluate the impact of the assimilation procedure at different horizontal resolutions and to assess the impact of assimilating reflectivity data from multiple radars, several experiments using Weather Research and Forecasting (WRF) model are performed. Finally, traditional verification scores as accuracy, equitable threat score, false alarm ratio and frequency bias, interpreted analyzing their uncertainty through bootstrap confidence intervals (CIs), are used to objectively compare the experiments, using rain gauge data as benchmark.

**Keywords:** radar data assimilation, WRF, 3D-Var, MET, bootstrap confidence intervals, HyMeX

## 1 Introduction

In the last few years, a large number of floods caused by different meteorological events occurred in Italy. These events mainly affected small areas (few hundreds of square kilometers) making their forecast very difficult. Indeed, one of the most important factors in producing a flash flood was found to be the persistence of the meteorological system over the

same area in the presence of specific hydrological conditions (the size of the drainage basin, the topography of the basin, the amount of urban use within the basin, and so on), allowing for accumulating large amount of rain (Doswell et al., 1996). In complex orography areas, such the Italian regions, this is largely due to the barrier effect produced by the mountains, such as the Apennines. Moreover, the Mediterranean basin is affected by a complex meteorology, due to the peculiar distribution of land and water and to the Mediterranean Sea temperature, which is warmer than that of the European northern seas (Baltic Sea and North Sea). These factors may produce severe meteorological events: for example, if precipitation persists over urbanized watersheds with steep slopes, devastating floods can occur in a relatively short time.

The scientific community widely recognizes the need of numerical weather prediction (NWP) models to be run at high resolution for improving very short term quantitative precipitation forecasts (QPF) during severe weather events and flash floods. The combination of NWP models and weather radar observations has shown improved skill with respect to extrapolation-based techniques (Sun et al., 2014). Nevertheless, the accuracy of the mesoscale NWP models is negatively affected by the "spin-up" effect (Daley 1991) and is mostly dependent on the errors in the initial and lateral boundary conditions (IC and BC, respectively), along with deficiencies in the numerical models themselves, and at the resolution of kilometers even more critical because of the lack of high resolution observations, beside for radar data. Several studies in the meteorological field have demonstrated that the assimilation of appropriate data into the NWP models, especially radar (Sugimoto et al., 2009) and satellite ones (Sokol, 2009), significantly reduces the "spin-up" effect and improves the IC and BC of the mesoscale models. Classical observations such as TEMP (upper level temperature, humidity, and winds observations) or SYNOP (surface synoptic observations) do not have enough density to describe for example local convection, while radar measurements can provide a sufficient density of data. Maiello et al. (2014) showed the positive effect of the assimilation of radar data into the precipitation forecast of a heavy rainfall event occurred in central Italy. The authors showed the gain by using assimilating radar data with respect to the conventional ones. Similar results are obtained for a case of severe convective storm in Croatia by Stanesic and Brewster (2016).

Weather radar has a fundamental role in showing tridimensional structures of convective storms and the associated mesoscale and microscale systems (Nakatani, 2015). As an example, Xiao and Sun (2007) showed that the assimilation of radar observation at high resolution (2km) can improve convective systems prediction. Recent researches in meteorology have established that the assimilation of real-time data, especially radar measurements (radial velocities and/or reflectivities), into the mesoscale NWP models can improve predicted precipitations for the next few hours. (e.g. Xiao et al., 2005; Sokol and Rezacova, 2006; Dixon et al., 2009; Salonen et al., 2010).

The aim of this study is to investigate the potential of improving NWP rainfall forecasts by assimilating multiple radar reflectivity data in combination or not with conventional observations. This may have a direct benefit also for hydrological applications, particularly for real time flash flood prediction and consequently for civil protection purposes. The novelty of the paper is in exploring the impact on the high-resolution forecast of the assimilation of multiple radar reflectivity data in a complex orography area, such as central Italian regions, to predict intense precipitation. This aim is reached by using the IOP4 of the SOP1 in the framework of the HyMeX campaign (Ducrocq et al. 2014, Ferretti et al. 2014, Davolio et al. 2015). The SOP1 was held from 5 September to 5 November 2012; the IOP4 was issued for the central Italy target area on 14 September 2012 and it was tagged both as a Heavy Precipitation Event (HPE) and a Flash Flood Event (FFE). The reflectivity measured by three C-band weather radars was ingested together with traditional meteorological observations (SYNOP and TEMP) using 3D-Var to improve WRF model

performance. So far, several studies about reflectivity data assimilation in heavy rainfall cases have been performed (e.g. Ha et al. 2011, Das et al. 2015) also including multiple radars data and in complex orography (e.g. Lee et al. 2010, Liu et al. 2013). However, this is the first experiment conducted on the Italian territory taking advantage of the reflectivity data collected by all the radars that cover central Italy.

The manuscript is arranged as follows. Section 2 provides information on the flash flood event and WRF model configuration. Section 3 presents the observations to be assimilated, the WRF 3D-Var data assimilation system, and the evaluation method used. The results are showed and assessed in the fourth Section. Summary and conclusions are reflected in the last Section.

## 2 Study area and model set up

Flash floods are still one of the natural hazards producing human and economic losses (Llasat et al. 2013). Moreover, an increasing trend of the occurrence of severe events in the whole Mediterranean area has been found by several authors (Hertig et al. 2012, Martin et al. 2013, Diodato and Bellocchi, 2014). These open issues drove the HyMeX programme (<http://www.hymex.org>) aims at a better understanding of the water cycle in the Mediterranean with focus on extreme weather events. The observation strategy of HyMeX is organized in a long-term (4 years) Enhanced Observation Periods (EOP) and short-term (2 months) Special Observation Periods (SOP). During the SOP1, that was held from 5 September to 5 November 2012 with the major aim of investigating still-unclear mesoscale meteorological mechanisms over the Mediterranean area, three Italian hydro-meteorological sites were identified within the Western Mediterranean Target Area (TA): Liguria–Tuscany (LT), northeastern Italy (NEI) and central Italy (CI). Several Intensive Observing Periods (IOPs) were issued during the campaign to document Heavy Precipitation Events (HPE), Flash Floods Events (FFE) and Orographic Precipitation Events (ORP).

### 2.1 Case study

During the day of 14 September 2012 a deep upper level trough entered the Mediterranean basin and deepened over the Tyrrhenian Sea slowly moving south eastward. A cut-off low developed over central Italy (Figure 1a, c) advecting cold air along the central Adriatic coast producing instability over central and southern Italy, and enhanced the Bora flow over the northern Adriatic Sea. Convection with heavy precipitations occurred in the morning of September 14 mainly along the central eastern Italian coast (Marche and Abruzzo regions), associated with the cut-off low over the Tyrrhenian Sea, producing flood in the urban area of Pescara where rainfall reached 150 mm in a few hours causing several river overflows, a landslide and many damages in the area of the city hospital. Progressive motion south-eastward of the cut-off and its filling (Figure 1b, d) gradually moved phenomena over south of Italy, even if some instability still remained over medium Adriatic until the afternoon of Saturday September 15. At the same time, a ridge developed high pressure on the west part of West Mediterranean domain; this ridge slowly drifts eastwards during the weekend.

Figure 2 shows the interpolated map of 24h accumulated rainfall recorded from rain gauges network from September 14 to September 15 (00:00-00:00UTC) with a maximum accumulated rainfall on the highest peak of Abruzzo region (Campo Imperatore) approximately reaching 300 mm in 24 hours. DEWETRA (Italian Civil Protection Department, CIMA Research Foundation, 2014) is an operational web platform used by the Italian Civil Protection Department (DPC) and implemented by CIMA Research Foundation (<http://www.cimafoundation.org/en/>). DEWETRA

allows synthesis, integration and comparison of information necessary for instrumental monitoring, models forecasting and to building real-time risk scenarios and their possible evolution. Rain gauges time series of some selected stations in Marche and Abruzzo regions, where most significant amount of rainfall is accumulated are presented in Figure 3: Fermo and Pintura di Bolognola (Marche region) respectively with nearly 130 mm in 24 hours (Figure 3a) and 180 mm in 24h (Figure 3b); Campo Imperatore, Atri and Pescara Colli (Abruzzo region) with respectively nearly 300 mm (Figure 3c), 160 mm (Figure 3d) and 140 mm (Figure 3e) in 24 hours. It is clearly shown (Figure 3) that the accumulation started around 02:00UTC of 14<sup>th</sup> September: in Fermo, Atri and Pescara Colli most of rainfall was concentrated in the first half of the day, whereas in Pintura di Bolognola and Campo Imperatore, precipitation fell all day long. The large amount of hourly precipitation for Atri and Pescara Colli respectively at 06:00UTC and 05:00UTC (red ovals in Fig. 3d and 3e) reaching 45mm/h, indicating convective precipitation, whereas rainfall at Campo Imperatore rain gauge (Fig. 3c) was much weaker but lasting longer which allowed for reaching an accumulated amount of approximately 300 mm in 24h.

Figure 4 shows the Vertical Maximum Intensity (VMI) reflectivity product from the Italian radar network (Vulpiani et al., 2008a) superimposed onto the Meteosat Second Generation (MSG) 10.8  $\mu$ m image (in normalized inverted greyscale). A zoom over the central Italy target area highlights a line of convective cells along the Apennines in central Italy due to the western flow approaching the orographic barrier. VMI values above 45 dBZ are associated with intense precipitation that occurred during convective events.

## 2.2 WRF model set up

The numerical weather prediction experiments are performed in this work using the non-hydrostatic Advanced Research WRF (ARW) modeling system V3.4.1. It is a primitive equations mesoscale meteorological model, with terrain-following vertical coordinates and options for different physical parameterizations. Skamarock et al. (2008) provides a detailed overview of the model.

In this study, a one-way nested configuration using the *ndown* program is used: a 12 km domain (263×185) that covers central Europe and west Mediterranean basin (referred as D01) is initialized using the European Centre for Medium-Range Weather Forecasts (ECMWF) analyses at 0.25 degrees of horizontal resolution; an innermost domain, that covers the whole Italy (referred as D02), with a grid space of 3 km (445×449) using as BC and IC the output of the previous forecast at 12 km. Both domains run with 37 unequally spaced vertical levels, from the surface up to 100 hPa (Figure 5).

Taking into account that the performance of a mesoscale model is highly related to the parameterization schemes, the main physics packages used in this study are set as for the operational configuration (Ferretti et al., 2014) used at the centre of Excellence CETEMPS. They include (Skamarock et al., 2008): the “New” Thompson et al. 2004 microphysics scheme, the MYJ (Mellor-Yamada-Janjic) scheme for the PBL (planetary boundary layer), the Goddard shortwave radiation scheme and the RRTM (rapid radiative transfer model) longwave radiation scheme, the Eta similarity scheme for surface layer formulation and the Noah LSM (Land Surface Model) to parameterize physics of land surface. A few preliminary tests are performed to assess the best cumulus parameterization scheme to be used both for the coarse and finest resolution domain for this event. Hence, the following parameterizations are tested: the new Kain–Fritsch and the Grell 3D schemes. The latter is an enhanced version of the Grell-Deveneyi scheme, in our simulations only used on the lowest resolution domain, where the option *cugd\_avedx* (subsidence spreading) is switched on. Based on the results of

these two cumulus parameterization schemes, the one producing the best precipitation forecast will be used to evaluate the impact of data assimilation.

### 3 Data and methodology

This section will be focused on the description of types of observations ingested into the assimilation procedure, namely both conventional and radar, and on the 3D-Var methodology as well as the observation operator used for the calculation of the reflectivity. Moreover, a brief overview of the evaluation method adopted to assess the performance of numerical weather predictions will be given.

#### 3.1 Observations to be assimilated

Conventional observations SYNOP and TEMP were retrieved from the ECMWF Meteorological Archival and Retrieval System (MARS). They have been packed in a suitable format for ingest into the assimilation procedure using the Observation Preprocessor (OBSPROC) module provided by the 3D-Var system. Among its main functions there are also to perform a quality control check and to assign observational errors based on a pre-specified error file. In short, a total of 983 observations (967 SYNOP and 16 TEMP) are ingested into the coarse resolution domain, whereas a total of 338 (333 SYNOP and 5 TEMP) observations into the high resolution one.

Reflectivity volumes taken from three C-band Doppler radars operational during the IOP4 have been assimilated to improve IC. The radars have different technical characteristics and were operated with different scanning strategies and operational settings as shown in Table 1.

Monte Midia (MM) and San Pietro Capofiume (SPC) radars are included in the Italian weather radar network, while Polar 55C (P55C) radar is a research radar working on demand, but was operational during the IOPs of the HyMeX campaign (Roberto et al., 2016).

It is worth mentioning that radar data can be affected by numerous sources of errors, mainly due to ground clutter, attenuation due to propagation or beam blocking, anomalous propagation and radio interferences. This is the reason why a preliminary "cleaning" procedure is applied to the measured radar reflectivity from the three radars before the assimilation process, consisting of the following 3 steps:

- a first quality check of radar volumes to filter out radar pixels affected by ground clutter and anomalous propagation. Furthermore,  $Z$  was corrected for attenuation using a methodology based on the specific differential phase shift ( $K_{dp}$ ) available for dual polarization radars (Vulpiani et al, 2015); moreover, reflectivity is not corrected for partial beam blocking: all the data that are affected by partial beam blocking and clutter have been filtered out;
- volume reflectivity radar data, for each elevation, are projected onto the Cartesian plane in order to find the closest radar bin for each Cartesian grid point and then they are interpolated by the 3D-Var code of WRF;
- the minimum assimilated reflectivity is set to -20 dBZ;

After the pre-processing procedure, a conversion from the native radar format into the one requested for the ingestion into the 3D-Var is applied to all radars reflectivity data.

Moreover, no observation thinning is performed because this procedure is not yet developed into the 3D-Var system for radar data. Nevertheless, a dynamical thinning has been devised that selects, for every assimilation cycle, the most influential partition of a particular measurement, from information based on the previous cycle: this is the multiple outer loops technique explained later in Section 4.

### 3.2 3D-Var data assimilation method

Data assimilation (DA) is a technique employed in many fields of geosciences perhaps most importantly in weather forecasting and hydrology. In this context it is the procedure by which observations are combined with the product (*first guess* or *background forecast*) of a NWP model and their corresponding error statistics, to produce a bettered estimate (the *analysis*) of the true state of the atmosphere (Skamarock et al., 2008). The variational DA method realizes this through the iterative minimization of a penalty function (Ide et al., 1997):

$$J(\mathbf{x}) = J^b(\mathbf{x}) + J^o(\mathbf{x}) = \frac{1}{2} \{ [\mathbf{y}^0 - H(\mathbf{x})]^T \mathbf{R}^{-1} [\mathbf{y}^0 - H(\mathbf{x})] + (\mathbf{x} - \mathbf{x}^b)^T \mathbf{B}^{-1} (\mathbf{x} - \mathbf{x}^b) \}, \quad (1)$$

where  $\mathbf{x}^b$  is the first guess state vector,  $\mathbf{y}^0$  is the assimilated observation vector,  $H$  is the observation operator that links the model variables to the observation variables and  $\mathbf{x}$  is the unknown analysis state vector to be found by minimizing  $J(\mathbf{x})$ . Finally,  $\mathbf{B}$  and  $\mathbf{R}$  are the background covariance error matrix and the observation covariance error matrix, respectively.

The minimization of the penalty function  $J(\mathbf{x})$ , displayed by Equation (1), is the a posteriori maximum likelihood estimate of the true atmosphere state, given the two sources of a priori data that are  $\mathbf{x}^b$  and  $\mathbf{y}^0$  (Lorenc, 1986).

In this study the 3D-Var system developed by Barker et al. (2003, 2004) is used for assimilating radar reflectivity and conventional observations SYNOP and TEMP. The penalty function minimization is performed in a preconditioned control variable space, where the preconditioned control variables are pseudo relative humidity, stream function, unbalanced temperature, unbalanced potential velocity and unbalanced surface pressure. Because of radar reflectivity assimilation is considered, the total water mixing ratio  $q_t$  is chosen as the moisture control variable. The following equation presents the observation operator used by the 3D-Var to calculate reflectivity for the comparison with the observed one (Sun and Crook, 1997):

$$Z = 43.1 + 17.5 \log(\rho q_r), \quad (2)$$

where  $\rho$  and  $q_r$  are the air density in  $\text{kg/m}^3$  and the rainwater mixing ratio in  $\text{g/kg}$ , respectively, while  $Z$  is the co-polar radar reflectivity factor expressed in dBZ. Since the total water mixing ratio  $q_t$  is used as the control variable, a warm rain process (Dudhia, 1989) is introduced into the WRF-3D-Var system to allow for producing the increments of moist variables linked to the hydrometeors.

The performance of the DA system strongly depends on the quality of the  $\mathbf{B}$  matrix in Equation (1). In this study, a specific background error statistics is computed for both domains for the entire SOPI duration using the National Meteorological Center (NMC) method (Parrish and Derber, 1992). This technique estimates the initial state error using differences of couples of forecasts valid at the same time, but with one of them having a delayed start time. One of the advantage of this method is that it maintains information on the dynamic of the model itself, but it may not give the proper correlation structure on data-sparse observations. Commonly, for regional applications and to remove the diurnal

cycle, a delay of 24 hours between the forecasts (T+24 minus T+12) is used; nevertheless, this delay can produce overestimated correlation length scales compared to those needed by a variational data assimilation technique, because of too dynamically evolved structures (Sadiki et al., 2000). Since 3D-Var is applied to the Mediterranean area,  $B$  has to take into account the scale of the motions of this orographic and meteorologically complex area: the model grid resolution ranges between 12 km and 3km, therefore the errors have to describe the physical phenomena relative to these scales.

### 3.3 Evaluation

The Point-Stat Tool of MET (Model Evaluation Tools) application (DTC, 2013), developed at the DTC (Developmental Testbed Center, NCAR), has been used to objectively evaluate the 12 hours accumulated precipitation produced by WRF on both domains. The interpolation method used to match the gridded model output to the point observation is the distance weighted mean in a 3 x 3 square of grid points. The observations used for the statistical evaluation were obtained from the DEWETRA platform of the Department of Civil Protection and the comparison has been performed over central Italy target area using about 3000 rain gauges with a good coverage throughout the Italian territory. Moreover, for interpreting results from the verification analysis bootstrap, confidence intervals (CIs) have been used to analyze the uncertainty associated with the score's values. Bootstrapping is a non parametric, computationally expensive, statistical technique (Efron & Tibshirani, 1993) for estimating parameters and uncertainty information, that allows to make inferences from data without making strong distributional assumptions about the data or the statistic being calculated. Therefore, the idea was to estimate CIs to set some bounds (bootstrap upper and lower confidence limits) on the expected value of the verification score helping to assess whether differences between competing forecasts are significant.

## 4 Design of the numerical experiments: discussion of the results

The simulations on the coarser resolution domain (D01) are run from 12:00UTC of 13 September 2012 and integrated for the following 96 hours, whereas runs on the finest resolution domain started at 00:00UTC of September 14 for a total of 48 hours of integration. The previous coarser resolution WRF forecast at 00:00UTC is used as the first guess in the 3D-Var experiment, because 00:00UTC has been selected as the "*analysis time*" of the assimilation procedure. After assimilation, the lateral and lower boundary conditions are updated for the high resolution forecast. Finally, the new IC and BC are used for the model initialization (in a warm start regime) at 00:00UTC. As already pointed out a set of preliminary experiments are performed using different cumulus convective scheme to assess the best one to be used. The following experiments are performed without assimilation and using the convective scheme on the coarser resolution domain only: KAIN-FRITSCH (KF\_MYJ); GRELL3D (GRELL3D\_MYJ); GRELL3D associated with the CUGD factor (GRELL3D\_MYJ\_CUGD). A summary of these numerical experiments is given in Table 2: the best performance is obtained by Grell3D scheme which is able to simulate the peak precipitation cumulated in 24 hours over Campo Imperatore, whereas KAIN-FRITSCH completely misses it (not shown here). The MET statistical analysis support the previous finding and the simulation with *cugd\_avedx* activated shows a significant performance in terms of uncertainty of the calculated scores than the other two simulations (not shown). Here after GRELL3D\_MYJ\_CUGD is referred as the control experiment (CTL) performed without any data assimilation.

At this point analysis of a new set of simulations is performed allowing to establish the best model configuration for the radar reflectivity assimilation. The DA experiments aim to investigate:

1. the impact of the assimilation at low and high resolution by assimilating both conventional and non-conventional data at both resolutions;
2. the impact of the assimilation of different types of observations;
3. the impact of the different radars, which is investigated by performing experiment by assimilating conventional data and then adding radar one by one.

Therefore in Table 3, together with CTL simulation, the following DA experiments are summarized: i) the assimilation of conventional data only (CON); ii) the assimilation of reflectivity data from MM only (CONMM) are added; iii) the assimilation of P55C radar reflectivity is added to the previous experiments (CONMMPOL); iv) the assimilation of the third radar reflectivity data is added to the previous (CONMMPOLSPC). Finally, an experiment to assess the role of the outer loop is performed (CONMMPOLSPC3OL): to include non-linearity into the observation operator and to evaluate the impact of reflectivity data entering for each cycle, the multiple outer loops strategy is applied (Rizvi et al., 2008). According to this approach, the non-linear problem is solved iteratively as a progression of linear problems: the assimilation system is able to ingest more observations by running more than one analysis outer loop.

In the following section the results will be presented and discussed following the rationale of the previously introduced experiments and analyzing the uncertainty (confidence level of 95%) in the realized scores (Forecast Accuracy (ACC), Frequency Bias (FBIAS), Equitable Threat Score (ETS), False Alarm Ratio (FAR)) for performance quantitative assessment.

## 5 Impact of conventional measurements and radar reflectivity assimilation on rainfall forecast: low versus high resolution

In figure 6, a preliminary comparison among low resolution (LR) simulations is shown. The control simulation (CTL) without data assimilation is shown in Figure 6a; whereas the other panels (b, c, d, e, f) show the experiments performed using the data assimilation.

Observing the outputs of different experiments (Fig. 6), best simulation is found for CONMMPOLSPC\_LR\_12KM (black arrow in Fig.6e): the rainfall maximum over Campo Imperatore is very well simulated, however a slight cell displacement at the border between Marche and Abruzzo regions is noticeable. The rain cumulated in 24 hours related to this cell is around 300 mm. In the simulations shown in Figures 6b and 6f, this cell is reproduced, although its position is shifted in another region. Furthermore, the precipitation pattern along the northern coasts of Abruzzo (black oval) is also quite well forecasted.

In Table 4 statistical indices ACC, FBIAS, ETS and FAR are reported, with their relative upper and lower confidence limits for the 12 hours accumulated precipitation and for two thresholds of precipitation, namely 1 mm and 40 mm, for light and heavy rain regimes, respectively. These two thresholds have been chosen due to their higher statistical significance than the other ones.

We obtained likely good values for ACC and FAR for all the experiments and for heavy rain regimes, strengthened by a small uncertainty interval. On the other hand, for the lower threshold it can be seen that for all simulations the values of FBIAS considering also the confidence intervals are greater than one. One possible interpretation of the impact of the

lower threshold, is that with 95% confidence all the experiments are overestimating the frequency of precipitation around 1 mm/12h.

Similarly to the above comparison, presented in figure 7 are high resolution results (HR) obtained performing reflectivity assimilation on 12 km domain (column 1), on 3 km (column 2) and on 12 km and 3 km together (column 3); to the top of figure 7 the CTL experiment on D02 is shown. Figure 7 is organized as follows: viewing panels by line, on line 1 all the simulations with conventional data assimilation only (CON\*) are found; on line 2 all the experiments with the assimilation of the reflectivity data from MM radar added (CONMM\*); on line 3 all the experiments with the assimilation of the reflectivity data from 2 C-band radars added (CONMMPOL\*); on line 4 all the experiments with the assimilation of the reflectivity data from all 3 C-band radars added (CONMMPOLSPC\*); on line 5 the simulations where the strategy of outer loop is adopted (CONMMPOLSPC3OL\*). In order to quantify the uncertainty associated to these experiments, the bootstrap 95% confidence intervals for verification statistics ACC, FBIAS, ETS, FAR have been summarized over tables (from 5 to 12) reporting again the two thresholds of precipitation: 1 mm/12h and 40 mm/12h (light and heavy rain regimes respectively).

In order to investigate the impact of the assimilation at different resolutions, we analyze figure 7 by column and comparing it with the available observations (Fig. 2) using also the statistical analysis:

- column 1 (12KM): CTL produces an overestimation of the rainfall that is not corrected by the assimilation of conventional data, but assimilating the reflectivity from the 3 radars and introducing the 3 outer loops (Fig. 7 column 1 line 5) the main cells are better reproduced. MET indices in Table 5 suggest that CTL and CON\_HR\_12KM have the widest spread between the CIs limits for higher thresholds, whereas CONMMPOLSPC3OL\_HR\_12KM is the simulation with the best response, secondly CONMM\_HR\_12KM, if we consider both the estimate of the scores and their uncertainty;
- column 2 (3KM): a partial correction of the rainfall overestimation compared to column 1 is observed especially if reflectivity from all the radars are assimilated and the outer loop strategy is applied; the statistical indices in Table 6 show CONMMPOLSPC3OL\_3KM as the best experiment among the assimilated ones because of competitive values of ACC at both thresholds and FBIAS and FAR for the light and heavy rain thresholds, respectively;
- column 3 (12KM\_3KM): rainfall overestimation was partially corrected compared to columns 1 and 2 by all the experiments; the MET statistics in Table 7 shows that CTL and CONMMPOLSPC3OL\_12KM\_3KM are the experiments with better values and small uncertainty, especially for ACC and ETS scores, although there is a quite broad spread in FBIAS of CTL experiment if we consider higher thresholds.

Summarizing, the previous analysis suggests that the frequency of rainfall overestimation for higher thresholds has been reduced by radar reflectivity assimilation performed only on D01. Furthermore, improvements come out for heavy rain regimes when radar reflectivity assimilation has been performed on the highest resolution domain, whereas the ingestion of conventional observations produces the worst results since a smaller number of them were assimilated into the finest resolution domain (for instance one sounding on five total) than that the coarser one. The assimilation, operated on both 12 km and 3 km, gives better results than the ones on column 1, but a worse response than the others on column 2 is given for higher thresholds.

In order to examine the impact of the assimilation of different data and radars, we can now analyze the experiments showed in figure 7 line by line. The results are compared with the observations of Fig. 2. The following considerations are worth discussing:

- line 1 (CON): a strong reduction of the rainfall is found with respect to CTL if conventional data are assimilated, but the rainfall pattern remains unchanged. Statistical indices of CON experiment (Table 8) do not improve the performances of CTL (despite a reduction in some cases of the spread between the CIs limits for higher thresholds of the FBIAS). The indices values suggest a slightly better performance when the conventional observations are assimilated only on the bigger domain and for higher thresholds, together with an improvement of FAR index for heavy rain regime;
- line 2 (CONMM): a further reduction in the precipitation overestimation is found as well as some variations in the pattern of the rainfall; the scores in Table 9, together with their bootstrap upper and lower limits, show that MM radar reflectivity and conventional observations assimilation, improves the model performance above all for lower thresholds respect to the experiments where only SYNOP and TEMP were ingested. It applies also for some of the scores at higher thresholds;
- line 3 (CONMMPOL): a quite strong improvement in the rainfall amount is found for all simulations. However, from the statistics of Table 10 we found a general worsening of the results both for light and heavy rain regimes when POL is added (ACC, FBIAS and ETS);
- line 4 (CONMMPOLSPC): a clear correction of the rainfall pattern is found; the overestimation produced by the simulation where the reflectivity from all the radars are assimilated on the 3 km domain has been corrected by the experiment in which the reflectivity is assimilated both on D01 and D02; the uncertainty in the realized scores of Table 11 suggests that the addition of SPC radar improves the results, furthermore they are not better than those where only MM is ingested;
- line 5 (CONMMPOLSPC3OL): the outer loop experiment confirms the strong overestimation reduction by \*12KM\_3KM; from Table 12 it seems that the introduction of 3OL improves the indices estimate and bounds above all when the 12 km domain is considered; CONMMPOLSPC3OL\_12KM\_3KM can be seen as the best simulation taking into account all the verification scores at both rainfall thresholds.

In summary, simulations results show that assimilation of conventional data is better to perform on the lowest resolution domain because more observations were used in the coarser domain, whereas when the assimilation is performed on the highest resolution domain only few SYNOP and even less TEMP fell down in the 3 km domain at the analysis time of the assimilation procedure. The impact of the conventional observations are expected to be lower than those of the non conventional ones, because most of them have already been used by ECMWF to produce their analysis and that they are here used as first guess, even if at lower resolution (0.25°). Therefore, they result to be correlated to the background and the improvements of those experiments where they are assimilated are expected to be low.

With regard to the assimilation of reflectivity radar data, should be noted that P55C radar observation is shielded at the lowest elevations by the Apennines. This leads to an underestimation of the precipitation, especially when the peak occurs; as a consequence a wrong estimation is given to the WRF model worsening the assimilation results. Also the outer loop strategy could have an important role in the assimilation procedure, but this latter needs a further investigation because a general rainfall underestimation for higher thresholds is found.

The results of this section confirm that when there is a correlation between the observations and the first guess used, the results of the data assimilation are poor, especially if no "special" observation is available on a wide area. The assimilation of a large amount of surface data together with the radiosonde ones decreases the quality of the final analysis produced. It probably depends on the different density of the surface and the three dimensional data of radiosondes, as assessed by Liu and Rabier (2002), being the former much larger than the latter.

## 6 Conclusions

In this manuscript the effects of multiple radar reflectivity data assimilation on a heavy precipitation event occurred during the SOP1 of the HyMeX campaign have been evaluated: the aim is to build a regionally-tuned numerical prediction model and decision-support system for environmental civil protection services within the central Italian regions. A sensitivity study at different domain resolution and using different types of data to improve initial conditions has been performed by assimilating into the WRF model radar reflectivity measurements, collected by three C-band Doppler weather radars operational during the event that hit central Italy on 14 September 2012. The 3D-Var and MET are the WRF tools used to assess this purpose. The study is performed on the complex basin, both for the orography and physical phenomena, of the Mediterranean area. First of all, WRF model responses to different types of cumulus parameterizations have been tested to establish the best configuration and to obtain the control simulation. The latter has been compared with observations and other experiments performed using 3D-Var. The set of assimilation experiments have been conducted following two different strategies: i) data assimilation at low and high resolution or at both resolutions simultaneously; ii) conventional data against radar reflectivity data assimilation. Both have been examined to assess the impact on rainfall forecast.

The major findings of this work have been the following:

- Grell 3D parameterization improves the simulations both on D01 and D02 and the use of the spreading factor is an added value in properly predict heavy rainfall over inland of Abruzzo and the rainfall pattern along the northeast coast;
- investigating the impact of the assimilation at different resolutions, best results are showed by the experiments where the data assimilation is performed on both domains 12 km and 3 km;
- the impact of the assimilation using different types of observations shows improvements if reflectivity from all the radars, along with SYNOP and TEMP are assimilated; furthermore, MM is the one that gives better results due to its excellent monitoring of the whole event;
- the outer loop strategy allows for further improving positive impact of the assimilation of multiple reflectivity radars data. Moreover, a deeper investigation of multiple outer loops strategy is required to well assess its impact, above all concerning the running time in an operational context;
- we have seen that there are thresholds where the WRF 3D-Var is statistically significant, with 95% confidence, while for other thresholds we have to be careful in drawing conclusions above all in the face of large uncertainty.

From the results obtained in this study, it is not possible to assess, in general terms, which is the best model configuration. In fact, this analysis should be performed systematically with a significant number of flash flood case studies. Nevertheless, this work has pointed out aspects in 3D-Var reflectivity data assimilation that encourages to

investigate more flash flood cases occurred over central Italy, in order to make the proposed approach suitable to provide a realistic prediction of possible flash floods both for the timing and localization of such events. To confirm and consolidate these initial findings, apart from analyzing more case studies, a deeper analysis of the meteorology of the region and of the performance of the data assimilation system throughout longer trials in a "pseudo-operational" procedure is necessary. **Moreover, a more sophisticated spatial verification technique (MODE, Method for Object-Based Diagnostic Evaluation, Davis et al., 2006a, 2006b) which focuses on the realism of the forecast, by comparing features or 'objects' that characterize both forecast and observation fields, could be investigated in the future. In fact, spatial verification methods are particularly suitable to address the model capability to reproduce structures like the convective systems responsible for the high precipitation events as considered in the present research, which, because of their typical dimensions, need high resolution simulations to be predicted (Gilleland et al., 2009). These new-generation spatial verification methods, through the identification and the geometrical description of 'objects' in forecast and observation fields (e.g. accumulated precipitation or radar reflectivity), permit an evaluation of the forecast skill in a more consistent way.**

### Acknowledgements

We are grateful to the Gran Sasso National Laboratories for support in computing resources, as well as the National Civil Protection Department and CIMA Research Foundation for rain gauges data using for the model validation. NCAR is also acknowledged for WRF model, 3D-Var system and MET tool. This work aims at contributing to the HyMeX programme.

### References

Barker, D.M., Huang, W., Guo, Y.-G., and Bourgeois, A.: A Three-Dimensional Variational (3D-Var) Data Assimilation System For Use With MM5. NCAR Tech. Note, NCAR/TN-453+STR, UCAR Communications, Boulder, CO, 68pp, 2003.

Barker, D.M., Huang, W., Guo, Y.-R., Bourgeois, A., and Xiao, Q.: A Three-Dimensional Variational (3D-Var) Data Assimilation System For Use With MM5: Implementation and Initial Results. *Mon. Wea. Rev.*, 132, 897-914, 2004.

Daley, R.: Atmospheric Data Analysis, Cambridge University Press, Cambridge, UK, 1991.

Das, M. K., M. A. M. Chowdhury, S. Das, S. K. Debsarma, and S. Karmakar: Assimilation of Doppler weather radar data and their impacts on the simulation of squall events during premonsoon season. *Natural Hazards*, 77(2), 901–931. DOI: 10.1007/s11069-015-1634-9, 2015.

**Davis A. C., Brown B., Bullock R.: Object-Based verification of precipitation forecasts. Part I: methodology and application to mesoscale rain areas. *Mon. Wea. Rev.* 134, 1772-1784, 2006a.**

**Davis A. C., Brown B., Bullock R.: Object-Based verification of precipitation forecasts. Part II: application to convective rain system. *Mon. Wea. Rev.* 134, 1785-1795, 2006b.**

Davolio, S., Ferretti, R., Baldini, L., Casaioli, M., Cimini, D., Ferrario, M. E., Gentile, S., Loglisci, N., Maiello, I., Manzato, A., Mariani, S., Marsigli, C., Marzano, F. S., Miglietta, M. M., Montani, A., Panegrossi, G., Pasi, F., Pichelli,

E., Pucillo, A. and Zinzi, A.: The role of the Italian scientific community in the first HyMeX SOP: an outstanding multidisciplinary experience. *Meteorologische Zeitschrift*, 24, 261-267, 2015.

Developmental Testbed Center, 2013: MET: Version 4.1 Model Evaluation Tools Users Guide. Available at <http://www.dtcenter.org/met/users/docs/overview.php>. 226 pp.

Diodato N. and Bellocchi G. (eds.), Storminess and Environmental Change, Advances in Natural and Technological Hazards Research 39, DOI 10.1007/978-94-007-7948-8\_2, *Springer Science+Business Media Dordrecht 2014*.

Dixon, M., Li, Z., Lean, H., Roberts, N., and Ballard, S.: Impact of data assimilation on forecasting convection over the United Kingdom using a high-resolution version of the Met Office Unified Model, *Mon. Weather Rev.*, 137, 1562–1584, 2009.

**Doswell C.A III., Brooks A.E., and Maddox R.A.: Flash Flood Forecasting: An Ingredients-Based Methodology. Weather and Forecasting, VOL. 11, 560-581, 1996.**

Ducrocq, V., Braud, I., Davolio, S., Ferretti, R., Flamant, C., Jansà, A., Kalthoff, N., Richard, E., Taupier-Letage, I., Ayral, P.-A., Belamari, S., Berne, A., Borga, M., Boudevillain, B., Bock, O., Boichard, J.-L., Bouin, M.-N., Bousquet, O., Bouvier, C., Chiggiato, J., Cimini, D., Corsmeier, U., Coppola, L., Cocquerez, P., Defer, E., Delanoë, J., Di Girolamo, P., Doerenbecher, A., Drobinski, P., Dufournet, Y., Fourrié, N., Gourley, J. J., Labatut, L., Lambert, D., Le Coz, J., Marzano, F. S., Molinié, G., Montani, A., Nord, G., Nuret, M., Ramage, K., Rison, B., Roussot, O., Said, F., Schwarzenboeck, A., Testor, P., Van-Baelen, J., Vincendon, B., Aran, M. and Tamayo, J.: HyMeX-SOP1, the field campaign dedicated to heavy precipitation and flash flooding in the northwestern Mediterranean. *Bulletin of the American Meteorological Society*, 95, 1083-1100, 2014.

Dudhia, J.: Numerical study of convection observed during the winter monsoon experiment using a mesoscale two-dimensional model, *J. Atmos. Sci.*, 46, 3077–3107, 1989.

**Efron, B. & R. J. Tibshirani: An Introduction to the Bootstrap. New York: Chapman and Hall, 1993.**

Ferretti, R., E. Pichelli, S. Gentile, I. Maiello, D. Cimini, S. Davolio, M. M. Miglietta, G. Panegrossi, L. Baldini, F. Pasi, F. S. Marzano, A. Zinzi, S. Mariani, M. Casaioli, G. Bartolini, N. Loglisci, A. Montani, C. Marsigli, A. Manzato, A. Pucillo, M. E. Ferrario, V. Colaiuda, and R. Rotunno: Overview of the first HyMeX Special Observation Period over Italy: observations and model results. *Hydr. Earth Syst. Sci.*, 18, 1953-1977, 2014, doi:10.5194/hess-18-1953-2014, 2014.

**Gilleland, E., Ahijevych, D., Brown, B.G., Casati, B., Ebert, E.E.: Intercomparison of spatial forecast verification methods. Weather Forecast. 24, 1416–1430, 2009.**

Ha, J.-H., H.-W. Kim, and D.-K. Lee: Observation and numerical simulations with radar and surface data assimilation for heavy rainfall over central Korea. *Advances in Atmospheric Sciences*, 28(3), 573–590. DOI: 10.1007/s00376-0100035-y, 2011.

Hertig E., Paxian A., Vogt G., Seubert S., Paeth H., Jacobbeit J.: Statistical and dynamical downscaling assessments of precipitation extremes in the Mediterranean area. *Meteorologische Zeitschrift*, Vol. 21 No. 1 , p. 61 - 77, 2012.

Ide, K., Courtier, P., Ghil, M., and Lorenc, A. C.: Unified notation for data assimilation: Operational, sequential and variational, *J. Meteorol. Soc. Jpn.*, 75, 181–189, 1997.

Italian Civil Protection Department and CIMA Research Foundation: The Dewetra Platform: A Multi-perspective Architecture for Risk Management during Emergencies. Springer International Publishing Switzerland, Chapter Information Systems for Crisis Response and Management in Mediterranean Countries, Volume 196 of the series Lecture Notes in Business Information Processing pp 165-177, 2014. DOI 10.1007/978-3-319-11818-5\_15

Llasat, M. C., Llasat-Botija, M., Petrucci, O., Pasqua, A. A., Rosselló, J., Vinet, F., and Boissier, L.: Towards a database on societal impact of Mediterranean floods within the framework of the HYMEX project, *Nat. Hazards Earth Syst. Sci.*, 13, 1337-1350, doi:10.5194/nhess-13-1337-2013, 2013.

Lee, J.-H., H.-H. Lee, Y. Choi, H.-W. Kim, and D.-K. Lee: Radar data assimilation for the simulation of mesoscale convective systems. *Advances in Atmospheric Sciences*, 27(5), 1025–1042. DOI: 10.1007/s00376-010-9162-8, 2010.

**Liu Z.-Q. and Rabier F.: The interaction between model resolution, observations resolution and observations density in data assimilation: a one-dimensional study. *Quart. J. Roy. Meteor. Soc.*, 128, 1367-1386, 2002.**

Liu, J., M. Bray, and D. Han: A study on WRF radar data assimilation for hydrological rainfall prediction. *Hydrology and Earth System Sciences*, 17(8), 3095–3110. DOI: 10.5194/hess-17-3095-2013, 2013.

Lorenc, A. C.: Analysis methods for numerical weather prediction, *Q. J. Roy. Meteorol. Soc.*, 112, 1177–1194, 1986.

Maiello, I., Ferretti, R., Gentile, S., Montopoli, M., Picciotti, E., Marzano, F. S., and Faccani, C.: Impact of radar data assimilation for the simulation of a heavy rainfall case in central Italy using WRF-3DVAR, *Atmos. Meas. Tech.*, 7, 2919-2935, doi:10.5194/amt-7-2919-2014, 2014.

Martín J. R., García M. M., Dávila F. de P., Soriano L. R.: Severe rainfall events over the western Mediterranean Sea: A case study. *Atmospheric Research*, 127, 47–63, 2013.

Nakatani T., Misumi R., Shoji Y., Saito K., Seko H., Seino N., Suzuki S-I., Shusse Y., Maesaka T., and Sugawara H. ; Tokyo metropolitan area convection study for extreme weather resilient cities. *BAMS*, 96, ES123-ES126, 2015.

Parrish, D.F. and Derber, J.C.: The National Meteorological Center's Spectral Statistical-Interpolation Analysis System. *Mon. Wea. Rev.*, 120, 1747-1763, 1992.

Rizvi, S., Guo, Y.-R., Shao, H., Demirtas, M., and Huang, X.-Y.: Impact of outer loop for WRF data assimilation system (WRFDA). 9th WRF Users' Workshop, Boulder, Colorado, 23-27 June 2008.

Roberto, N., Adirosi, E., Baldini, L., Casella, D., Dietrich, S., Gatlin, P., Panegrossi, G., Petracca, M., Sanò, P., and Tokay, A.: Multi-sensor analysis of convective activity in central Italy during the HyMeX SOP 1.1, *Atmos. Meas. Tech.*, 9, 535-552, doi:10.5194/amt-9-535-2016, 2016.

**Sadiki W., Fischer C. and Geleyn J.-F.: Mesoscale Background Error Covariances: Recent Results Obtained with the Limited-Area Model ALADIN over Morocco. *Mon. Wea. Rev.*, 128, 3927-3935, 2000.**

Salonen K, Haase G, Eresmaa R, Hohti H, Järvinen H.: Towards the operational use of Doppler Radar radial winds in HIRLAM. *Atmospheric Research* 100: 190–200, 2010.

Skamarock, W.C., Klemp, J.B., Dudhia, J., Gill, D.O., Barker, D.M., Duda, M. G., Huang, X.-Y., Wang, W., and Powers, J. G.: A description of the Advanced Research WRF Version 3. NCAR Technical Note. TN 475+STR, 113 pp., available from [www.mmm.ucar.edu/wrf/users/docs/arw\\_v3.pdf](http://www.mmm.ucar.edu/wrf/users/docs/arw_v3.pdf) (last access: January 2012), 2008.

Sokol, Z. and Rezacova, D.: Assimilation of Radar reflectivity into the LMCOSMO model with a high horizontal resolution, *Meteorol. Appl.*, 13, 317–330, 2006.

Sokol, Z.: Effects of an assimilation of Radar and satellite data on a very short range forecast of heavy convective rainfalls, *Atmos. Res.*, 93, 188–206, 2009.

Stanesic A., and K.A. Brewester: Impact of Radar Data Assimilation on the Numerical Simulation of a Severe Storm in Croatia. *Met.Zeit.* Vol. 25, No. 1, 37–53, 2016

Sugimoto, S., Crook N.A., Sun J., Xiao Q., and Barker D.M.: An examination of WRF 3D-VarRadar data assimilation on its capability in retrieving unobserved variables and forecasting precipitation through observing system simulation experiments. *Mon. Wea. Rev.*, 137, 4011-4029, 2009. DOI:10.1175/2009MWR2839.1.

Sun, J. Xue, M., Wilson J. W., Zawadzki I., Ballard S.P., Onvlee-Hooimeyer J., Joe P., Barker D.M., Li P-W., Golding B., Xu M., and Pinto J.: Use of NWP for nowcasting convective precipitation, recent progress and challenges. *BAMS*, 95, 409-426, 2014.

Sun, J. and Crook, N.A.: Dynamical and Microphysical Retrieval from Doppler RADAR Observations Using a Cloud Model and Its Adjoint. Part I: Model Development and Simulated Data Experiments. *J. Atmos. Sci.*, 54, 1642-1661, 1997.

Thompson, G., R. M. Rasmussen, and K. Manning: Explicit forecasts of winter precipitation using an improved bulk microphysics scheme. Part I: Description and sensitivity analysis. *Mon. Wea. Rev.*, 132, 519–542, 2004.

Vulpiani G., Pagliara, P., Negri, M., Rossi, L., Gioia, A., Giordano, P. P., Alberoni, P. P., Cremonini, R., Ferraris, L., and Marzano, F. S.: The Italian radar network within the national early-warning system for multi-risks management, Proc. of Fifth European Conference on Radar in Meteorology and Hydrology (ERAD 2008), 184, Finnish Meteorological Institute, Helsinki, 30 June-4 July, 2008a.

Vulpiani, G., Baldini, L., and Roberto, N.: Characterization of Mediterranean hail-bearing storms using an operational polarimetric X-band radar, *Atmos. Meas. Tech.*, 8, 4681-4698, doi:10.5194/amt-8-4681-2015, 2015.

Xiao, Q., Kuo, Y.-H., Sun, J. and Lee, W.-C.: Assimilation of Doppler RADAR Observations with a Regional 3D-Var System: Impact of Doppler Velocities on Forecasts of a Heavy Rainfall Case. *J. Appl. Meteor.*, 44, 768-788, 2005.

Xiao, Q. and Sun, J.: Multiple-RADAR Data Assimilation and Short-Range Quantitative Precipitation Forecasting of a Squall Line Observed during IHOP\_2002. *Mon. Wea. Rev.*, 135, 3381-3404, 2007.

## LIST OF FIGURES

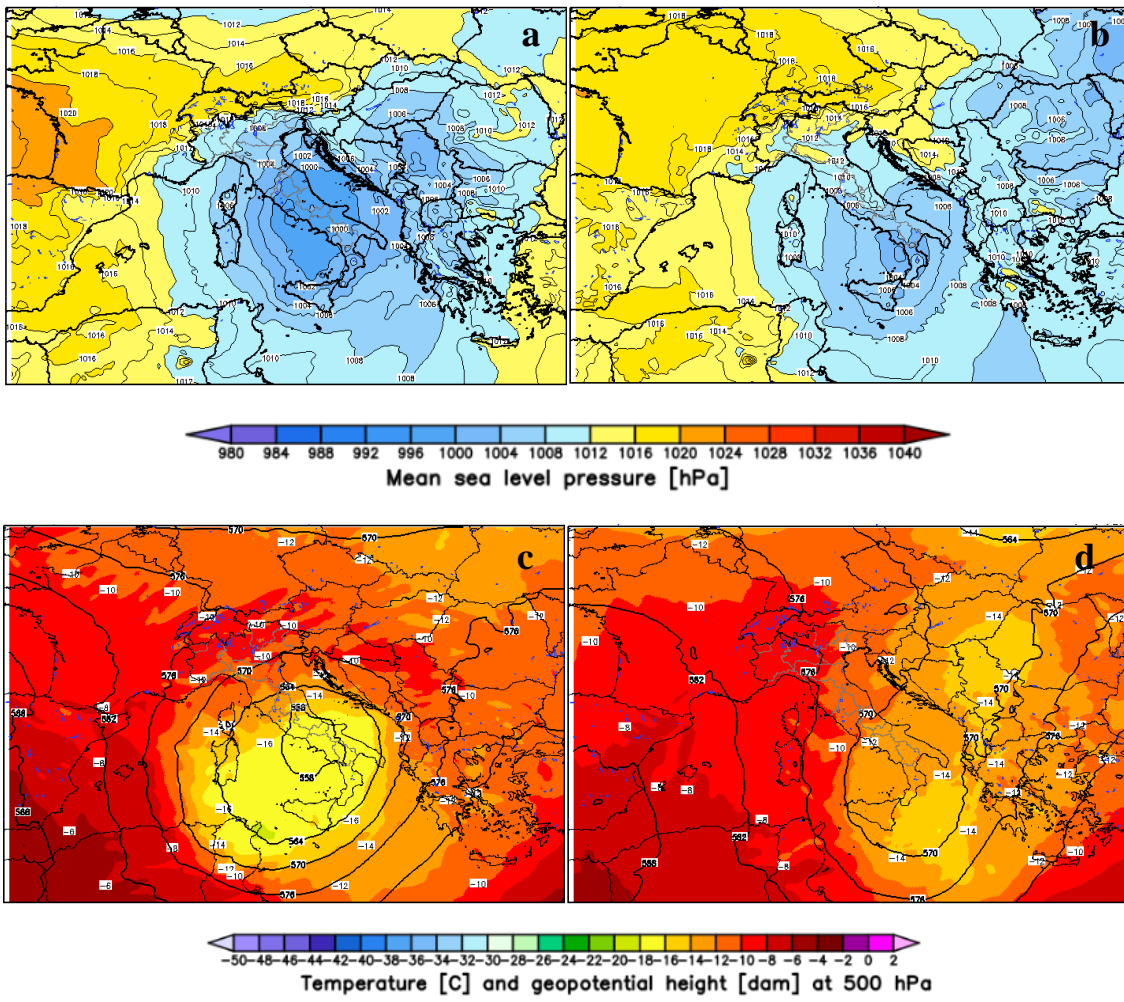


**Figure 1.** ECMWF (European Center for Medium-Range Weather Forecasts) analyses at 12:00UTC on 14 September 2012: a) mean sea level pressure, c) temperature (color shades) and geopotential height (black isolines) at 500 hPa; ECMWF analyses at 12:00UTC on 15 September 2012: b) mean sea level pressure, d) temperature (black isolines) and geopotential height (color shades) at 500 hPa.

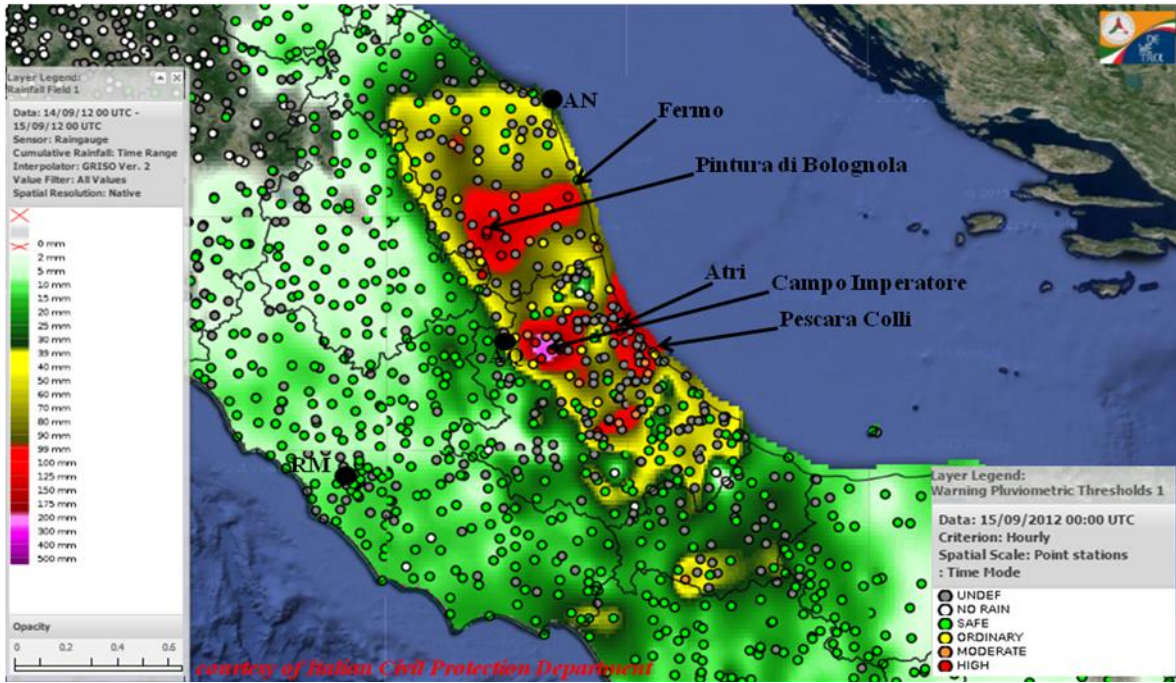
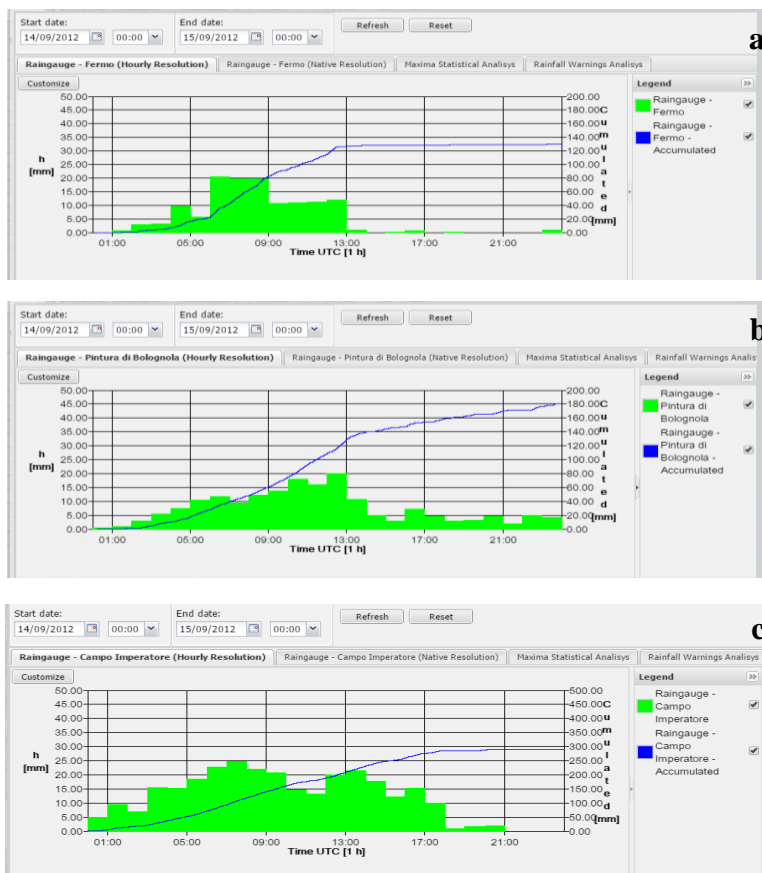
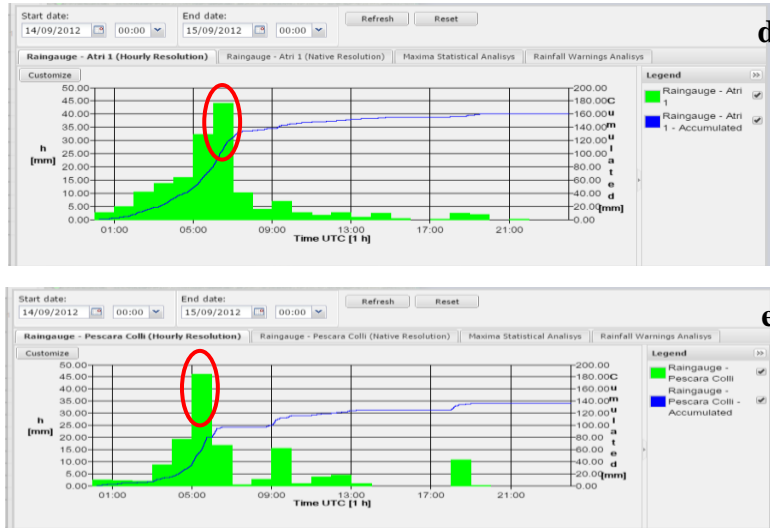
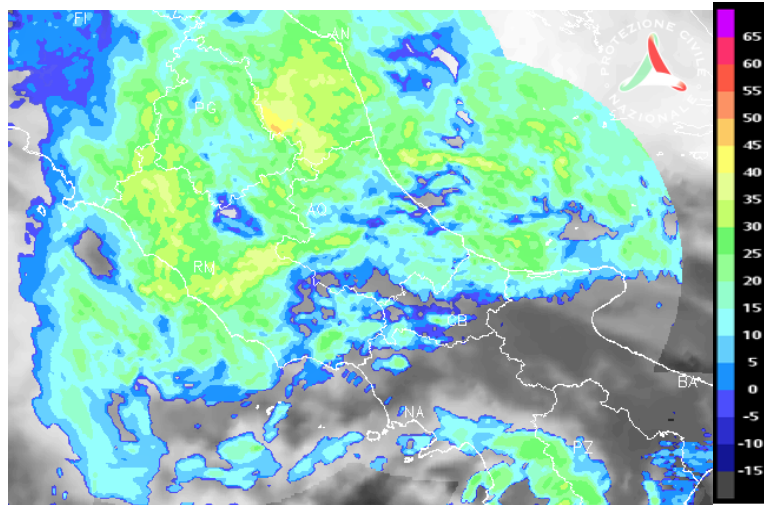


Figure 2: Interpolated map of 24h accumulated rainfall from 00:00UTC of 14 September 2012 over Abruzzo and Marche regions taken from DEWETRA system from rain gauges measurements.  
Black contours are the administrative boundaries of regions, while the colored circles represent the warning pluviometric thresholds.

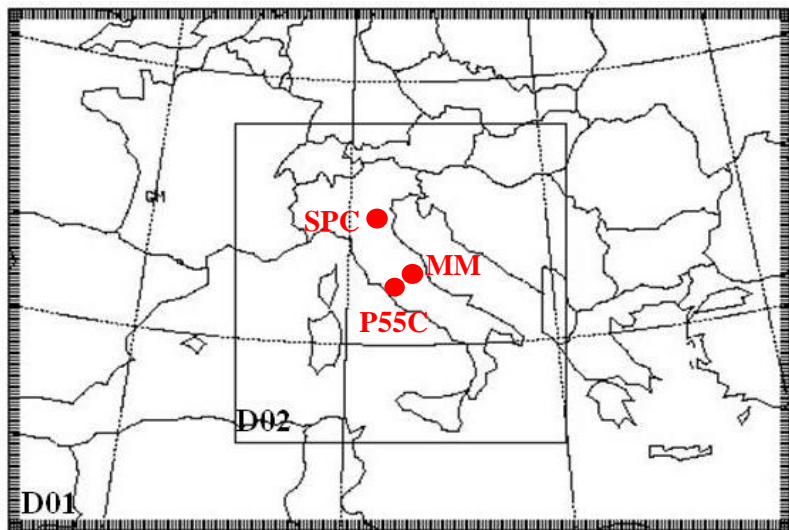




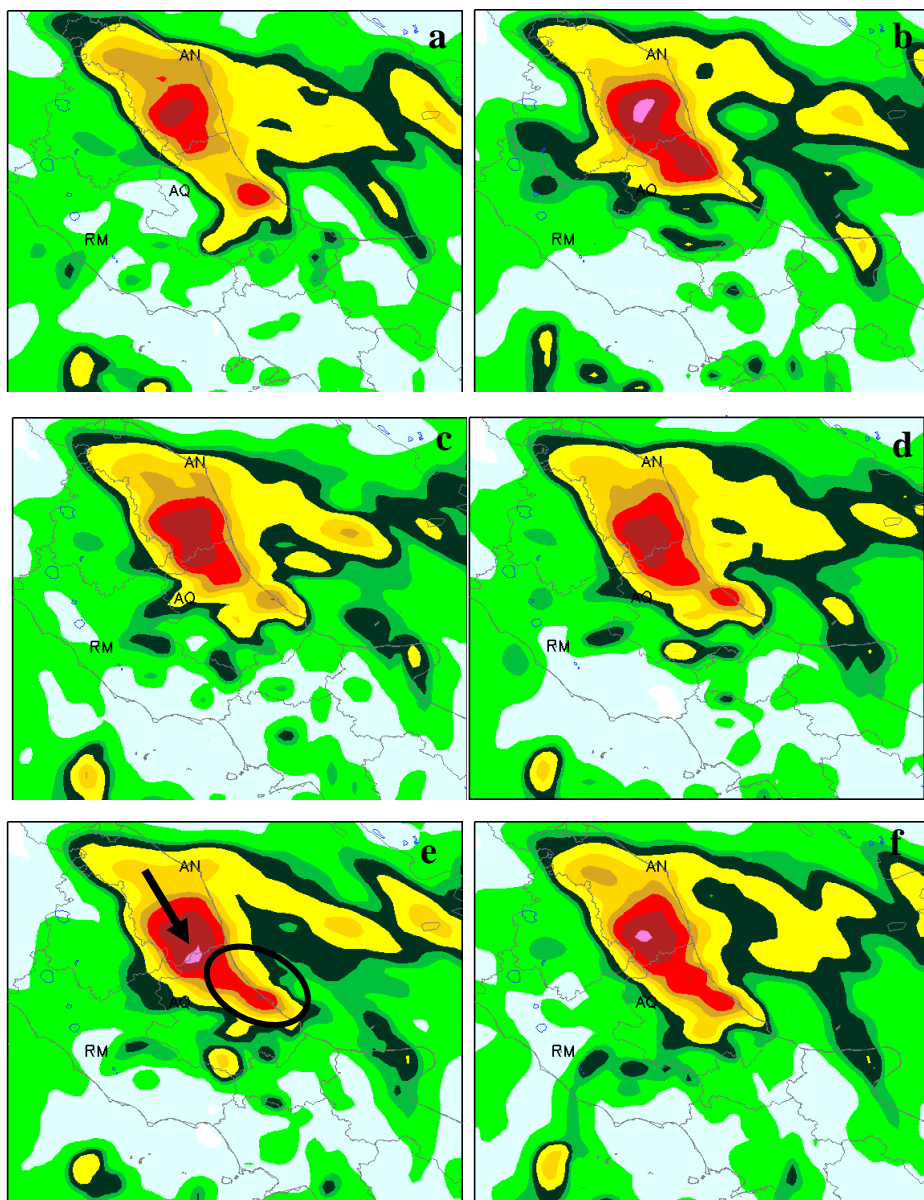
**Figure 3: Rain gauges time series of some selected stations in Marche (a, Fermo and b, Pintura di Bolognola) and Abruzzo (c, Campo Imperatore, d, Atri and e, Pescara Colli) regions during the event of 14 September 2012. The green histogram represents the hourly accumulated precipitation (scale on the left); the blue line represents the incremental accumulation within the 24h (scale on the right). (courtesy of Italian Civil Protection Department)**



**Figure 4: Zoom over central Italy of the reflectivity on 14 September 2012 at 08:00UTC from the Italian radar network overlapped with the MSG (IR 10.8) at 07:30UTC. (courtesy of Italian DPC)**

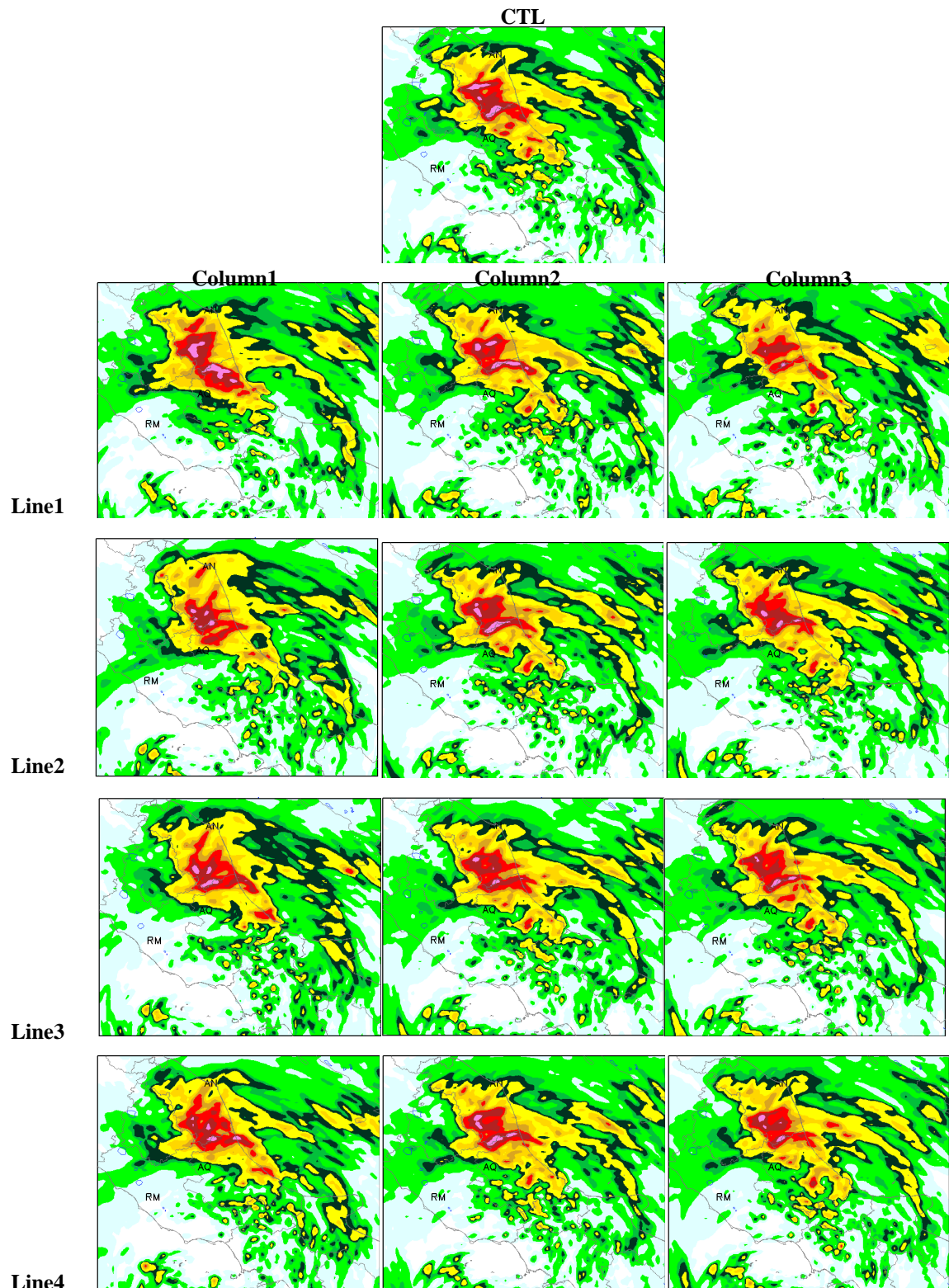


**Figure 5: WRF ndown domains configuration: the two domains have respectively resolution of 12km and 3km. The high resolution D02 over Italy includes Mt. Midia (MM), ISAC-CNR (P55C) and San Pietro Capofiume (SPC) radars (red dots in the figure).**





**Figure 6: WRF D01 accumulated 24h rainfall forecast over central Italy from 00:00UTC of 14 September 2012: a) WRF D01 CTL; b) WRF D01 CON\_LR\_12KM; c) WRF D01 CONMM\_LR\_12KM; d) WRF D01 CONMMPOL\_LR\_12KM; e) WRF D01 CONMMPOLSPC\_LR\_12KM; f) WRF D01 CONMMPOLSPC3OL\_LR\_12KM.**



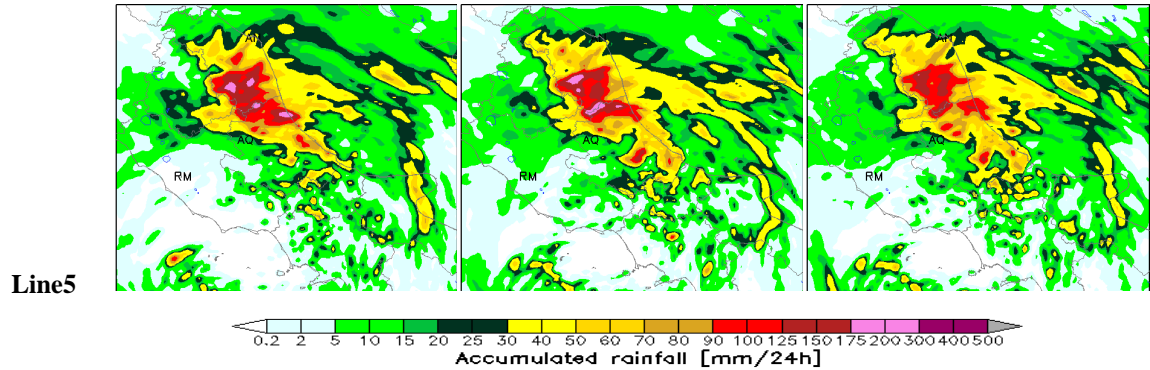


**Figure 7:** WRF D02 accumulated 24h rainfall forecast over central Italy from 00:00UTC of 14 September 2012: CTL simulation (top center); on each column simulations obtained performing reflectivity assimilation at different resolutions (\*12KM, \*3KM, \*12KM\_3KM); on each line simulations performed assimilating different kinds of data (CON\*, CONMM\*, CONMMPOL\*, CONMMPOLSPC\*, CONMMPOLSPC3OL\*).

**Table 1: Technical characteristics of the three radars whose reflectivity have been assimilated during IOP4.**

Features	Units	MM radar	P55C radar	SPC radar
Owner		CF Abruzzo Region	ISAC-CNR of Rome	Arpa Emilia Romagna
Location		Monte Midia	Rome	San Pietro Capofiume
Latitude	[deg]	42.057	41.840	44.6547
Longitude	[deg]	13.177	12.647	11.6236
Height (a.s.l.)	[m]	1760	130	31
Doppler		YES	YES	YES
Dual Polarization		NO	YES	YES
Range Resolution	[m]	500	75	250
Temporal Resolution	[min]	15	5	15
Number of PPI scans	[#]	4 (0, 1, 2, 3)	6 or 8 (0.6, 1.6, 2.6, 4.4, 6.2, 8.3, 11.0, 14.6)	6 (0.53, 1.4, 2.3, 3.2, 4.15, 5.0)
Maximum Range	[km]	120 or 240	125	125

**Table 2: List of experiments to assess the cumulus parameterization.**

Experiment	Cumulus	Grid Resolution	Assimilation Synop+Temp	Assimilation Radar
KF_MYJ	KAIN-FRITSCH	12KM/3KM	NO	NO
GRELL3D_MYJ	GRELL3D	12KM/3KM	NO	NO
GRELL3D_MYJ_CUGD (CTL)	GRELL3D+CUGD	12KM/3KM	NO	NO

**Table 3: List of experiments to test the impact of data assimilation.**

Experiment	Cumulus	Grid Resolution	Assimilation Synop+Temp	Assimilation Radar
CTL	GRELL3D+CUGD	12KM/3KM	NO	NO
CON	GRELL3D+CUGD	12KM/3KM/BOTH	YES	NO
CONMM	GRELL3D+CUGD	12KM/3KM/BOTH	YES	MM
CONMMPOL	GRELL3D+CUGD	12KM/3KM/BOTH	YES	MM+POL
CONMMPOLSPC	GRELL3D+CUGD	12KM/3KM/BOTH	YES	MM+POL+SPC
CONMMPOLSPC3OL	GRELL3D+CUGD	12KM/3KM/BOTH	YES	MM+POL+SPC with 3 outer loops

**Table 4: Bootstrap 95% confidence intervals for verification statistics Forecast Accuracy (ACC), Frequency Bias (FBIAS), Equitable Threat Score (ETS), False Alarm Ratio (FAR). They are considered as a function of thresholds (1mm/12h and 40mm/12h). The experiments are: CTL, CON\_LR\_12KM, CONMM\_LR\_12KM, CONMMPOL\_LR\_12KM, CONMMPOLSPC\_LR\_12KM, CONMMPOLSPC3OL\_LR\_12KM.**

Experiment	ACC		FBIAS		ETS		FAR	
	Thresholds mm/12h	40						
CTL	(0.78) <b>0.82</b> (0.86)	(0.96) <b>0.98</b> (0.99)	(1.21) <b>1.40</b> (1.68)	(0.03) <b>0.07</b> (0.12)	(0.20) <b>0.29</b> (0.39)	(0.01) <b>0.03</b> (0.05)	(0.31) <b>0.37</b> (0.43)	(0) <b>0.002</b> (0.004)
CON_LR_12KM	(0.81) <b>0.85</b> (0.88)	(0.96) <b>0.98</b> (0.99)	(1.22) <b>1.41</b> (1.66)	(0.06) <b>0.12</b> (0.23)	(0.26) <b>0.36</b> (0.46)	(0.02) <b>0.04</b> (0.07)	(0.26) <b>0.32</b> (0.38)	(0.001) <b>0.004</b> (0.007)
CONMM_LR_12KM	(0.79) <b>0.83</b> (0.87)	(0.97) <b>0.98</b> (0.99)	(1.18) <b>1.37</b> (1.62)	(0.12) <b>0.20</b> (0.28)	(0.21) <b>0.30</b> (0.41)	(0.09) <b>0.16</b> (0.22)	(0.31) <b>0.37</b> (0.43)	(0) <b>0.002</b> (0.003)
CONMMPOL_LR_12KM	(0.79) <b>0.83</b> (0.87)	(0.97) <b>0.98</b> (0.99)	(1.23) <b>1.43</b> (1.70)	(0.13) <b>0.21</b> (0.28)	(0.21) <b>0.31</b> (0.41)	(0.10) <b>0.16</b> (0.23)	(0.29) <b>0.36</b> (0.42)	(0) <b>0.002</b> (0.003)
CONMMPOLSPC_LR_12KM	(0.79) <b>0.83</b> (0.87)	(0.97) <b>0.98</b> (0.99)	(1.25) <b>1.44</b> (1.73)	(0.08) <b>0.15</b> (0.24)	(0.23) <b>0.32</b> (0.43)	(0.05) <b>0.11</b> (0.18)	(0.28) <b>0.35</b> (0.41)	(0) <b>0.002</b> (0.003)
CONMMPOLSPC3OL_LR_12KM	(0.78) <b>0.82</b> (0.86)	(0.97) <b>0.98</b> (0.99)	(1.21) <b>1.39</b> (1.65)	(0.10) <b>0.18</b> (0.27)	(0.21) <b>0.30</b> (0.40)	(0.06) <b>0.13</b> (0.20)	(0.32) <b>0.38</b> (0.44)	(0) <b>0.002</b> (0.004)

**Table 5: Bootstrap 95% confidence intervals for verification statistics Forecast Accuracy (ACC), Frequency Bias (FBIAS), Equitable Threat Score (ETS), False Alarm Ratio (FAR) and referred to experiments in column 1. They are considered as a function of thresholds (1mm/12h and 40mm/12h). The experiments are: CTL, CON\_HR\_12KM, CONMM\_HR\_12KM, CONMMPOL\_HR\_12KM, CONMMPOLSPC\_HR\_12KM, CONMMPOLSPC3OL\_HR\_12KM.**

Experiment	ACC		FBIAS		ETS		FAR	
	Thresholds mm/12h		Thresholds mm/12h		Thresholds mm/12h		Thresholds mm/12h	
	1	40	1	40	1	40	1	40
CTL	(0.79) 0.83 (0.87)	(0.96) 0.98 (0.99)	(0.79) 0.94 (1.13)	(0.14) 0.47 (1.61)	(0.23) 0.33 (0.45)	(0.04) 0.10 (0.16)	(0.16) 0.21 (0.27)	(0.001) 0.007 (0.15)
CON_HR_12KM	(0.77) 0.81 (0.84)	(0.96) 0.97 (0.99)	(0.75) 0.91 (1.11)	(0.21) 0.49 (1.61)	(0.15) 0.25 (0.36)	(0.03) 0.07 (0.13)	(0.20) 0.26 (0.31)	(0.005) 0.011 (0.019)
CONMM_HR_12KM	(0.78) 0.82 (0.86)	(0.97) 0.98 (0.99)	(0.79) 0.95 (1.16)	(0.15) 0.29 (0.64)	(0.18) 0.28 (0.39)	(0.07) 0.14 (0.21)	(0.19) 0.24 (0.31)	(0.000) 0.004 (0.008)
CONMMPOL_HR_12KM	(0.76) 0.80 (0.84)	(0.96) 0.98 (0.99)	(0.66) 0.82 (1.01)	(0.07) 0.14 (0.25)	(0.10) 0.20 (0.30)	(0.03) 0.06 (0.12)	(0.20) 0.25 (0.31)	(0.001) 0.003 (0.006)
CONMMPOLSPC_HR_12KM	(0.78) 0.82 (0.86)	(0.96) 0.98 (0.99)	(0.71) 0.86 (1.05)	(0.08) 0.22 (0.59)	(0.18) 0.28 (0.39)	(0.02) 0.06 (0.12)	(0.16) 0.21 (0.27)	(0.001) 0.005 (0.011)
CONMMPOLSPC3OL_HR_12KM	(0.78) 0.82 (0.86)	(0.96) 0.98 (0.99)	(0.77) 0.93 (1.13)	(0.13) 0.31 (0.86)	(0.20) 0.30 (0.41)	(0.04) 0.10 (0.17)	(0.14) 0.20 (0.26)	(0.002) 0.006 (0.012)

**Table 6: Bootstrap 95% confidence intervals for verification statistics Forecast Accuracy (ACC), Frequency Bias (FBIAS), Equitable Threat Score (ETS), False Alarm Ratio (FAR) and referred to experiments in column 2. They are considered as a function of thresholds (1mm/12h and 40mm/12h). The experiments are: CTL, CON\_3KM, CONMM\_3KM, CONMMPOL\_3KM, CONMMPOLSPC\_3KM, CONMMPOLSPC3OL\_3KM.**

Experiment	ACC		FBIAS		ETS		FAR	
	Thresholds mm/12h		Thresholds mm/12h		Thresholds mm/12h		Thresholds mm/12h	
	1	40	1	40	1	40	1	40
CTL	(0.80) 0.83 (0.87)	(0.96) 0.98 (0.99)	(0.79) 0.94 (1.13)	(0.14) 0.47 (1.61)	(0.23) 0.33 (0.45)	(0.04) 0.10 (0.16)	(0.16) 0.21 (0.27)	(0.001) 0.007 (0.15)
CON_3KM	(0.78) 0.82 (0.85)	(0.96) 0.98 (0.99)	(0.65) 0.80 (0.98)	(0.08) 0.18 (0.42)	(0.14) 0.24 (0.35)	(0.03) 0.06 (0.12)	(0.17) 0.22 (0.28)	(0.001) 0.004 (0.009)
CONMM_3KM	(0.78) 0.82 (0.86)	(0.97) 0.98 (0.99)	(0.79) 0.96 (1.17)	(0.14) 0.31 (0.68)	(0.17) 0.26 (0.37)	(0.05) 0.13 (0.26)	(0.18) 0.24 (0.29)	(0.001) 0.005 (0.11)
CONMMPOL_3KM	(0.77) 0.81 (0.85)	(0.96) 0.98 (0.99)	(0.76) 0.94 (1.16)	(0.12) 0.28 (0.65)	(0.13) 0.23 (0.33)	(0.03) 0.09 (0.14)	(0.18) 0.24 (0.30)	(0.001) 0.006 (0.11)

CONMMPOLSPC_3KM	(0.78) <b>0.82</b> (0.86)	(0.96) <b>0.98</b> (0.99)	(0.85) <b>1.03</b> (1.25)	(0.10) <b>0.27</b> (0.83)	(0.18) <b>0.28</b> (0.39)	(0.03) <b>0.07</b> (0.13)	(0.19) <b>0.24</b> (0.31)	(0.001) <b>0.005</b> (0.012)
CONMMPOLSPC3OL_3KM	(0.79) <b>0.83</b> (0.86)	(0.97) <b>0.98</b> (0.99)	(0.81) <b>0.96</b> (1.17)	(0.10) <b>0.24</b> (0.64)	(0.17) <b>0.27</b> (0.39)	(0.05) <b>0.12</b> (0.19)	(0.21) <b>0.27</b> (0.33)	(0.000) <b>0.003</b> (0.007)

**Table 7: Bootstrap 95% confidence intervals for verification statistics Forecast Accuracy (ACC), Frequency Bias (FBIAS), Equitable Threat Score (ETS), False Alarm Ratio (FAR) and referred to experiments in column 3. They are considered as a function of thresholds (1mm/12h and 40mm/12h). The experiments are: CTL, CON\_12KM\_3KM, CONMM\_12KM\_3KM, CONMMPOL\_12KM\_3KM, CONMMPOLSPC\_12KM\_3KM, CONMMPOLSPC3OL\_12KM\_3KM.**

Experiment	ACC Thresholds mm/12h		FBIAS Thresholds mm/12h		ETS Thresholds mm/12h		FAR Thresholds mm/12h	
	1	40	1	40	1	40	1	40
CTL	(0.80) <b>0.83</b> (0.87)	(0.96) <b>0.98</b> (0.99)	(0.79) <b>0.94</b> (1.13)	(0.14) <b>0.47</b> (1.61)	(0.23) <b>0.33</b> (0.45)	(0.04) <b>0.10</b> (0.16)	(0.16) <b>0.21</b> (0.27)	(0.001) <b>0.007</b> (0.015)
CON_12KM_3KM	(0.77) <b>0.81</b> (0.84)	(0.96) <b>0.98</b> (0.99)	(0.68) <b>0.84</b> (1.03)	(0.02) <b>0.10</b> (0.34)	(0.11) <b>0.20</b> (0.30)	(0.01) <b>0.04</b> (0.007)	(0.21) <b>0.27</b> (0.33)	(0) <b>0.001</b> (0.004)
CONMM_12KM_3KM	(0.79) <b>0.83</b> (0.86)	(0.96) <b>0.98</b> (0.99)	(0.79) <b>0.96</b> (1.18)	(0.09) <b>0.31</b> (1.02)	(0.18) <b>0.28</b> (0.40)	(0.03) <b>0.07</b> (0.13)	(0.17) <b>0.23</b> (0.29)	(0.001) <b>0.006</b> (0.013)
CONMMPOL_12KM_3KM	(0.77) <b>0.81</b> (0.85)	(0.96) <b>0.98</b> (0.99)	(0.79) <b>0.96</b> (1.19)	(0.11) <b>0.26</b> (0.65)	(0.14) <b>0.23</b> (0.33)	(0.03) <b>0.08</b> (0.14)	(0.19) <b>0.25</b> (0.31)	(0.001) <b>0.006</b> (0.011)
CONMMPOLSPC_12KM_3KM	(0.77) <b>0.81</b> (0.85)	(0.97) <b>0.98</b> (0.99)	(0.87) <b>1.04</b> (1.28)	(0.09) <b>0.25</b> (0.70)	(0.16) <b>0.26</b> (0.37)	(0.04) <b>0.08</b> (0.14)	(0.22) <b>0.28</b> (0.34)	(0) <b>0.004</b> (0.009)
CONMMPOLSPC3OL_12KM_3KM	(0.79) <b>0.83</b> (0.86)	(0.97) <b>0.98</b> (0.99)	(0.82) <b>0.98</b> (1.18)	(0.08) <b>0.15</b> (0.24)	(0.19) <b>0.30</b> (0.41)	(0.05) <b>0.11</b> (0.18)	(0.19) <b>0.25</b> (0.31)	(0) <b>0.002</b> (0.003)

**Table 8: Bootstrap 95% confidence intervals for verification statistics Forecast Accuracy (ACC), Frequency Bias (FBIAS), Equitable Threat Score (ETS), False Alarm Ratio (FAR) and referred to experiments in line 1. They are considered as a function of thresholds (1mm/12h and 40mm/12h). The experiments are: CTL, CON\_3KM, CON\_HR\_12KM, CON\_12KM\_3KM.**

Experiment	ACC Thresholds mm/12h		FBIAS Thresholds mm/12h		ETS Thresholds mm/12h		FAR Thresholds mm/12h	
	1	40	1	40	1	40	1	40
CTL	(0.80) <b>0.83</b> (0.87)	(0.96) <b>0.98</b> (0.99)	(0.79) <b>0.94</b> (1.13)	(0.14) <b>0.47</b> (1.61)	(0.23) <b>0.33</b> (0.45)	(0.04) <b>0.10</b> (0.16)	(0.16) <b>0.21</b> (0.27)	(0.001) <b>0.007</b> (0.014)

CON_3KM	(0.78) <b>0.82</b> (0.85)	(0.96) <b>0.98</b> (0.99)	(0.65) <b>0.80</b> (0.98)	(0.08) <b>0.18</b> (0.42)	(0.14) <b>0.24</b> (0.35)	(0.03) <b>0.06</b> (0.12)	(0.17) <b>0.22</b> (0.28)	(0.001) <b>0.004</b> (0.009)
CON_HR_12KM	(0.77) <b>0.81</b> (0.85)	(0.96) <b>0.97</b> (0.99)	(0.75) <b>0.91</b> (1.11)	(0.21) <b>0.49</b> (1.61)	(0.15) <b>0.25</b> (0.36)	(0.03) <b>0.07</b> (0.13)	(0.20) <b>0.26</b> (0.31)	(0.005) <b>0.0011</b> (0.19)
CON_12KM_3KM	(0.77) <b>0.81</b> (0.84)	(0.96) <b>0.98</b> (0.99)	(0.68) <b>0.84</b> (1.03)	(0.02) <b>0.10</b> (0.34)	(0.11) <b>0.20</b> (0.30)	(0.01) <b>0.04</b> (0.07)	(0.21) <b>0.27</b> (0.33)	(0) <b>0.001</b> (0.004)

**Table 9: Bootstrap 95% confidence intervals for verification statistics Forecast Accuracy (ACC), Frequency Bias (FBIAS), Equitable Threat Score (ETS), False Alarm Ratio (FAR) and referred to experiments in line 2. They are considered as a function of thresholds (1mm/12h and 40mm/12h). The experiments are: CTL, CONMM\_3KM, CONMM\_HR\_12KM, CONMM\_12KM\_3KM.**

Experiment	ACC		FBIAS		ETS		FAR	
	Thresholds mm/12h		Thresholds mm/12h		Thresholds mm/12h		Thresholds mm/12h	
	1	40	1	40	1	40	1	40
CTL	(0.80) <b>0.83</b> (0.87)	(0.96) <b>0.98</b> (0.99)	(0.79) <b>0.94</b> (1.13)	(0.14) <b>0.47</b> (1.61)	(0.23) <b>0.33</b> (0.45)	(0.04) <b>0.10</b> (0.16)	(0.16) <b>0.21</b> (0.27)	(0.001) <b>0.007</b> (0.15)
CONMM_3KM	(0.78) <b>0.82</b> (0.86)	(0.97) <b>0.98</b> (0.99)	(0.79) <b>0.96</b> (1.17)	(0.14) <b>0.31</b> (0.68)	(0.17) <b>0.26</b> (0.37)	(0.05) <b>0.13</b> (0.26)	(0.18) <b>0.24</b> (0.29)	(0.001) <b>0.005</b> (0.011)
CONMM_HR_12KM	(0.78) <b>0.82</b> (0.86)	(0.97) <b>0.98</b> (0.99)	(0.79) <b>0.95</b> (1.16)	(0.15) <b>0.29</b> (0.64)	(0.18) <b>0.28</b> (0.39)	(0.07) <b>0.14</b> (0.21)	(0.19) <b>0.24</b> (0.31)	(0) <b>0.004</b> (0.008)
CONMM_12KM_3KM	(0.79) <b>0.83</b> (0.86)	(0.96) <b>0.98</b> (0.99)	(0.79) <b>0.96</b> (1.18)	(0.09) <b>0.31</b> (1.01)	(0.18) <b>0.28</b> (0.40)	(0.03) <b>0.07</b> (0.13)	(0.17) <b>0.23</b> (0.29)	(0.001) <b>0.006</b> (0.013)

**Table 10: Bootstrap 95% confidence intervals for verification statistics Forecast Accuracy (ACC), Frequency Bias (FBIAS), Equitable Threat Score (ETS), False Alarm Ratio (FAR) and referred to experiments in line 3. They are considered as a function of thresholds (1mm/12h and 40mm/12h). The experiments are: CTL, CONMMPOL\_3KM, CONMMPOL\_HR\_12KM, CONMMPOL\_12KM\_3KM.**

Experiment	ACC		FBIAS		ETS		FAR	
	Thresholds mm/12h		Thresholds mm/12h		Thresholds mm/12h		Thresholds mm/12h	
	1	40	1	40	1	40	1	40
CTL	(0.79) <b>0.83</b> (0.87)	(0.96) <b>0.98</b> (0.99)	(0.79) <b>0.94</b> (1.13)	(0.14) <b>0.47</b> (1.61)	(0.23) <b>0.33</b> (0.45)	(0.04) <b>0.10</b> (0.16)	(0.16) <b>0.21</b> (0.27)	(0.001) <b>0.007</b> (0.15)
CONMMPOL_3KM	(0.77) <b>0.81</b> (0.85)	(0.96) <b>0.98</b> (0.99)	(0.76) <b>0.94</b> (1.16)	(0.12) <b>0.28</b> (0.65)	(0.13) <b>0.23</b> (0.33)	(0.03) <b>0.09</b> (0.14)	(0.18) <b>0.24</b> (0.30)	(0.001) <b>0.006</b> (0.011)

CONMMPOL_HR_12KM	(0.76) <b>0.80</b> (0.84)	(0.97) <b>0.98</b> (0.99)	(0.66) <b>0.82</b> (1.01)	(0.07) <b>0.14</b> (0.25)	(0.10) <b>0.20</b> (0.30)	(0.03) <b>0.006</b> (0.11)	(0.20) <b>0.25</b> (0.31)	(0.001) <b>0.003</b> (0.006)
CONMMPOL_12KM_3KM	(0.77) <b>0.81</b> (0.85)	(0.96) <b>0.98</b> (0.99)	(0.79) <b>0.96</b> (1.19)	(0.11) <b>0.26</b> (0.65)	(0.14) <b>0.23</b> (0.33)	(0.03) <b>0.08</b> (0.13)	(0.19) <b>0.25</b> (0.31)	(0.01) <b>0.005</b> (0.011)

**Table 11:** Bootstrap 95% confidence intervals for verification statistics Forecast Accuracy (ACC), Frequency Bias (FBIAS), Equitable Threat Score (ETS), False Alarm Ratio (FAR) and referred to experiments in line4. They are considered as a function of thresholds (1mm/12h and 40mm/12h). The experiments are: CTL, CONMMPOLSPC\_3KM, CONMMPOLSPC\_HR\_12KM, CONMMPOLSPC\_12KM\_3KM.

Experiment	ACC		FBIAS		ETS		FAR	
	Thresholds mm/12h		Thresholds mm/12h		Thresholds mm/12h		Thresholds mm/12h	
	1	40	1	40	1	40	1	40
CTL	(0.79) <b>0.83</b> (0.87)	(0.96) <b>0.98</b> (0.99)	(0.79) <b>0.94</b> (1.13)	(0.14) <b>0.47</b> (1.61)	(0.23) <b>0.33</b> (0.45)	(0.04) <b>0.10</b> (0.16)	(0.16) <b>0.21</b> (0.27)	(0.001) <b>0.007</b> (0.015)
CONMMPOLSPC_3KM	(0.78) <b>0.82</b> (0.86)	(0.96) <b>0.98</b> (0.99)	(0.85) <b>1.03</b> (1.25)	(0.10) <b>0.27</b> (0.83)	(0.18) <b>0.28</b> (0.39)	(0.03) <b>0.07</b> (0.13)	(0.19) <b>0.25</b> (0.31)	(0.001) <b>0.005</b> (0.012)
CONMMPOLSPC_HR_12KM	(0.78) <b>0.82</b> (0.86)	(0.96) <b>0.98</b> (0.99)	(0.71) <b>0.86</b> (1.05)	(0.08) <b>0.22</b> (0.59)	(0.17) <b>0.28</b> (0.39)	(0.02) <b>0.06</b> (0.12)	(0.16) <b>0.21</b> (0.27)	(0.001) <b>0.005</b> (0.11)
CONMMPOLSPC_12KM_3KM	(0.77) <b>0.81</b> (0.85)	(0.96) <b>0.98</b> (0.99)	(0.87) <b>1.04</b> (1.28)	(0.09) <b>0.25</b> (0.70)	(0.16) <b>0.26</b> (0.36)	(0.04) <b>0.08</b> (0.14)	(0.22) <b>0.28</b> (0.34)	(0) <b>0.004</b> (0.009)

**Table 12:** Bootstrap 95% confidence intervals for verification statistics Forecast Accuracy (ACC), Frequency Bias (FBIAS), Equitable Threat Score (ETS), False Alarm Ratio (FAR) and referred to experiments in line 5. They are considered as a function of thresholds (1mm/12h and 40mm/12h). The experiments are: CTL, CONMMPOLSPC3OL\_3KM, CONMMPOLSPC3OL\_HR\_12KM, CONMMPOLSPC3OL\_12KM\_3KM.

Experiment	ACC		FBIAS		ETS		FAR	
	Thresholds mm/12h		Thresholds mm/12h		Thresholds mm/12h		Thresholds mm/12h	
	1	40	1	40	1	40	1	40
CTL	(0.79) <b>0.83</b> (0.87)	(0.96) <b>0.98</b> (0.99)	(0.79) <b>0.94</b> (1.13)	(0.14) <b>0.47</b> (1.61)	(0.23) <b>0.33</b> (0.44)	(0.04) <b>0.10</b> (0.16)	(0.16) <b>0.21</b> (0.27)	(0.001) <b>0.007</b> (0.015)
CONMMPOLSPC3OL_3KM	(0.79) <b>0.83</b> (0.86)	(0.97) <b>0.98</b> (0.99)	(0.81) <b>0.96</b> (1.17)	(0.10) <b>0.24</b> (0.64)	(0.17) <b>0.27</b> (0.39)	(0.05) <b>0.12</b> (0.19)	(0.21) <b>0.27</b> (0.33)	(0) <b>0.003</b> (0.007)
CONMMPOLSPC3OL_HR_12KM	(0.78) <b>0.82</b> (0.82)	(0.96) <b>0.98</b> (0.98)	(0.77) <b>0.93</b> (0.93)	(0.13) <b>0.31</b> (0.31)	(0.20) <b>0.30</b> (0.30)	(0.004) <b>0.10</b> (0.14)	(0.14) <b>0.20</b> (0.20)	(0.002) <b>0.006</b> (0.006)

	(0.86)	(0.99)	(1.13)	(0.86)	(0.41)	(0.17)	(0.26)	(0.012)
CONMMPOLSPC3OL_12KM_3KM	(0.79) <b>0.83</b> (0.86)	(0.97) <b>0.98</b> (0.99)	(0.82) <b>0.98</b> (1.18)	(0.08) <b>0.15</b> (0.24)	(0.19) <b>0.30</b> (0.41)	(0.04) <b>0.11</b> (0.18)	(0.19) <b>0.25</b> (0.31)	(0) <b>0.002</b> (0.003)